

# Robustness Beyond Known Groups with Low-rank Adaptation

Abinitha Gourabathina<sup>1</sup> Hyewon Jeong<sup>1</sup> Teya Bergamaschi<sup>1</sup> Marzyeh Ghassemi<sup>1</sup> Collin Stultz<sup>1,2</sup>

## Abstract

Deep learning models trained to optimize average accuracy often exhibit systematic failures on particular subpopulations. In real world settings, the subpopulations most affected by such disparities are frequently unlabeled or unknown, thereby motivating the development of methods that are performant on sensitive subgroups without being pre-specified. However, existing group-robust methods typically assume prior knowledge of relevant subgroups, using group annotations for training or model selection. We propose Low-rank Error Informed Adaptation (LEIA), a simple two-stage method that improves group robustness by identifying a low-dimensional subspace in the representation space where model errors concentrate. LEIA restricts adaptation to this error-informed subspace via a low-rank adjustment to the classifier logits, directly targeting latent failure modes without modifying the backbone or requiring group labels. Using five real-world datasets, we analyze group robustness under three settings: (1) truly no knowledge of subgroup relevance, (2) partial knowledge of subgroup relevance, and (3) full knowledge of subgroup relevance. Across all settings, LEIA consistently improves worst-group performance while remaining fast, parameter-efficient, and robust to hyperparameter choice. Our code is available at [this repository](#).

## 1. Introduction

As deep neural networks (DNNs) are trained with the goal of high average accuracy, they are not guaranteed to be performant with respect to any particular subgroup (Tsipras et al., 2019; Shah et al., 2020; Raghavan et al., 2020). This is particularly problematic for high-stakes decision making, such

<sup>1</sup>Department of Electrical Engineering & Computer Science, Massachusetts Institute of Technology, Cambridge, MA, USA

<sup>2</sup>Harvard School of Medicine, Harvard, Boston, MA, USA. Correspondence to: Collin Stultz <cmstultz@mit.edu>.

Preprint. February 9, 2026.

as hiring (Raghavan et al., 2020; Wilson & Caliskan, 2024), detecting hate speech (Sap et al., 2019), and predicting disease diagnoses (Obermeyer et al., 2019; Banerjee et al., 2023), where predictions must be both accurate and unbiased across sensitive attributes to prevent the perpetuation of existing societal inequities. Failures of models to generalize to certain subpopulations can arise from several factors (Yang et al., 2023), including spurious correlations (Geirhos et al., 2020), where non-causal features erroneously influence predictions; attribute imbalance (Martinez et al., 2021), in which the attribute distributions shifts between training and test time; class imbalance (Liu et al., 2019), where class label proportions cause models to prioritize the majority; and attribute generalization (Santurkar et al., 2020), when models encounter previously unseen attribute values at test time.

Many existing approaches for improving robustness across subpopulations require access to both group labels (which specify the group attribute) and class labels on the training data (Sagawa et al., 2020; Idrissi et al., 2021). This requirement is limiting in the real world, where such group labels may be expensive to obtain (Sohoni et al., 2020; Liu et al., 2021; Buolamwini & Gebru, 2018), noisy (Kruppal, 2013; Awasthi et al., 2020), or missing (Kallus et al., 2022; Lahoti et al., 2020). Moreover, use of explicit group optimization strategies presupposes *a priori* knowledge of relevant subgroups, which is not a realistic assumption. For instance, in clinical settings, the relevance of subgroups evolves with medical knowledge: early cardiovascular risk models did not account for zip code, which is now recognized as an important proxy for environment and socioeconomic status (Musaogullari et al., 2025).

Alarmingly, presupposing the subgroups of importance and training models to perform well on these particular subgroups may result in *worse* performance on unseen or unknown subgroups (Kaplow & Shavell, 1999; Kearns et al., 2018; Kleinberg et al., 2018; Hashimoto et al., 2018). More recent methods do not rely on group labels during training (Liu et al., 2021; Zhang et al., 2022; Qiu et al., 2023), but often use labels in the validation set for hyperparameter tuning and early stopping, which is unrealistic for real-world deployment, where complete relevant group information is likely not available or known with certainty.

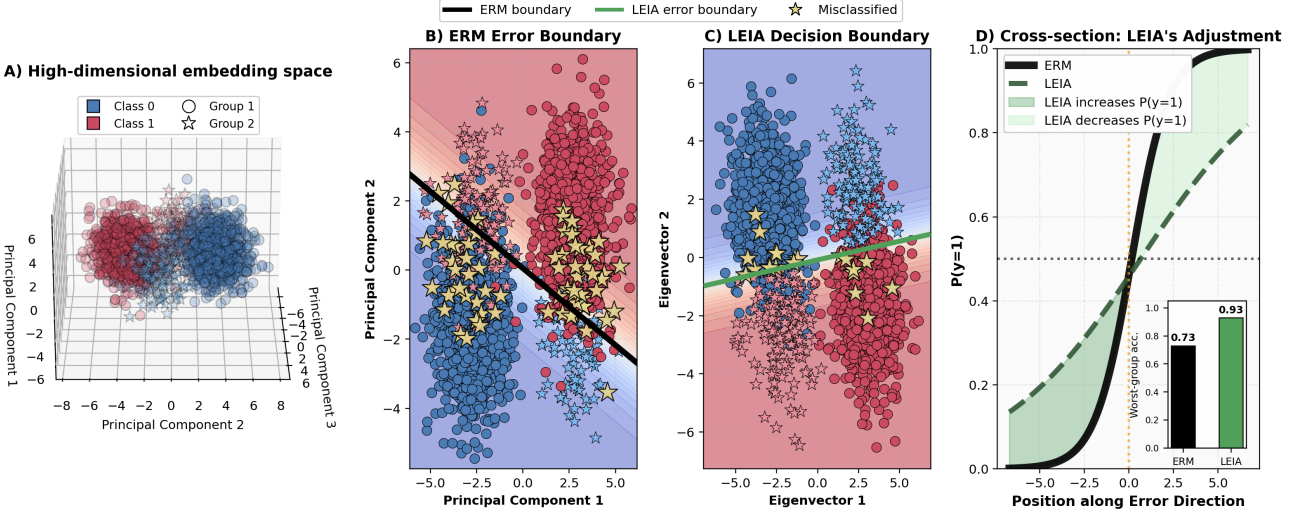


**Figure 1. Low-rank Error Informed Adaptation in action.** After training with ERM, LEIA adjusts ERM’s decision boundary along a low-rank error subspace. A) High dimensional embedding space projected in three dimensions via PCA, showing an entangled cluster of binary classification problem with two subgroups ( $\circ$ ) and ( $\star$ ). B) and C) ERM’s boundary in the high variance directions compared to LEIA’s adjusted boundary in the identified error direction (eigenvectors). Yellow stars indicate misclassified points of the worst-performing subgroup. D) Probability adjustments according to the identified principal eigenvector. Samples from the worst group ( $\star$ ) that are initially misclassified with ERM are corrected by LEIA directly in logit space. We show the improved worst group accuracy in this synthetic data setup.

In this paper, we propose **Low-rank Error Informed Adaptation (LEIA)**, a simple and efficient method for group robustness with minimal computational overhead beyond standard training. As in prior two-stage approaches (Kirichenko et al., 2022; Qiu et al., 2023), we freeze the feature extractor of a base model trained via empirical risk minimization (ERM) and focus adaptation on the final classification layer. However, rather than relying on explicit subgroup annotations, LEIA adopts a geometric perspective on model errors. Using a weighted loss on a held-out subset of the training data, where weights emphasize examples on which the base model incurs high loss, LEIA identifies a low-dimensional *error informed subspace* in the representation space. Adaptation is then restricted to this subspace via a low-rank additive adjustment to the classifier logits. We illustrate the LEIA method in Figure 1. The main contributions of this work are:

1. We motivate the importance of assessing group robustness methods with unknown subgroups qualitatively, theoretically, and empirically.
2. We propose LEIA, an approach for improving robustness without requiring explicit subgroup annotations. By directly targeting the geometry of the model’s error patterns, LEIA mitigates latent subgroup errors that standard ERM and group-based methods fail to address, resulting in consistent gains in worst-group performance.
3. We empirically validate LEIA using five real-world datasets, showing state-of-the-art performance in settings with (1) no knowledge of subgroup relevance, (2)

partial knowledge of subgroup relevance, and (3) full knowledge of subgroup relevance. LEIA is faster and more parameter-efficient than other baselines, making it practical for large models and resource-constrained settings. Moreover, LEIA’s data-driven hyperparameter selection significantly improving group robustness without careful tuning.

## 2. Related Work

A growing body of literature focuses on group robustness to assess whether models learn meaningful feature relationships and achieve equitable performance (Yang et al., 2023). Traditional ERM training, however, has been shown to learn misleading shortcuts (McCoy et al., 2019; Ribeiro et al., 2016; Beery et al., 2018; Zech et al., 2018; Winkler et al., 2019; Shahamatdar et al., 2024), causing performance gaps in subpopulations (Zhao et al., 2017; Banerjee et al., 2023).

Many existing methods for group robustness assume access to labeled relevant subgroups or attributes (Sagawa et al., 2020; Arjovsky & Bottou, 2017) or on a subset of the available data used to train the parameters of the model (Kirichenko et al., 2022; Yao et al., 2022). Such access is often unrealistic given how labels may be expensive to obtain, noisy, or missing. Moreover, relevant groups may be unknown.

Recent work has explored the setting of assuming access to all subgroups during validation. These methods commonly train an initial ERM model and then retrain a classifier with

balanced classes (Kang et al., 2020), upweighting misclassified samples (Liu et al., 2021; Nam et al., 2020), or contrastive learning (Zhang et al., 2022). A prominent paradigm of second stage classifier retraining is group inference from the representations of the initial ERM. Prior approaches infer groups from clustered representations (Sohoni et al., 2020), identifying violations of the invariant risk minimization (IRM) objective, a trained spurious attribute classifier (Han & Zou, 2024), and ensemble models (To et al., 2025). Instead of retraining a full classifier, Automatic Feature Reweighting (AFR) (Qiu et al., 2023) is a fast method that retrains only the last layer of a standard ERM-trained base model. However, many of these methods are evaluated assuming full knowledge of group relevancy in the validation set, ignoring scenarios where some groups are unknown a priori.

Our method also draws on prior work that established how biases can be mitigated with low dimensions in transformers and vision language models (Zhao et al., 2025; Jang et al., 2025; Chuang et al., 2023; Jung et al., 2024; Gerych et al., 2024; Zhao et al., 2025). Additionally, parameter-efficient adaptation techniques such as low-rank updates (LoRA) (Hu et al., 2022) have shown that task- or subgroup-specific improvements can be achieved by updating only a small fraction of model parameters (Hu et al., 2022; Rimsky et al., 2024; Wu et al., 2024; Yin et al., 2024).

We provide an extended discussion of related work in Appendix F.

### 3. The Importance of Unknown Groups

A central challenge in robust machine learning is that the relevance of subpopulations may be *unknown* at training time. We define unknown subgroups as groups that may be seen in the training dataset, but are unknown as an important or relevant subgroup for which to optimize performance. This phenomenon can stem from missing group labels during training time (Sohoni et al., 2020) or not knowing which groups are actually relevant. For example, early clinical trials of beta-blockers predominantly enrolled male participants, as clinical outcomes on women were ignored, leading to treatment guidelines that later proved less effective, and in some cases harmful, for women (Vogel et al., 2021; Mas-Llado et al., 2023; Rossello et al., 2025). Similar post-hoc discoveries of vulnerable subpopulations arise in pharmacogenomics (Martin et al., 2017), diagnostic imaging (Oakden-Rayner et al., 2019), and public health (McCoy et al., 2024), where biological, demographic, or contextual factors interact in complex and previously unrecognized ways. In high-stakes domains like medicine, subgroup effects are routinely appreciated only after widespread adoption, thereby delaying their acceptance as reasonable metrics that one should use to gauge robust performance.

### 3.1. Group-Based Training Methods Can Falter with Incomplete Subgroup Knowledge

**Problem setup.** Let  $\mathcal{X}$  and  $\mathcal{Y}$  denote the input and label spaces, and let  $\ell : \mathcal{X} \times \mathcal{Y} \rightarrow \mathbb{R}_+$  be a loss function. Data are drawn from an unknown distribution  $\mathcal{D}$  over  $\mathcal{X} \times \mathcal{Y}$ , and  $\mathcal{H}$  denotes a hypothesis class. We assume the population admits a latent partition into disjoint subgroups  $\mathcal{G} = \{G_1, \dots, G_K, G^*\}$ , where all subgroups are present in the training distribution, but only  $G_1, \dots, G_K$  are *identified* and *explicitly optimized for* during training. The subgroup  $G^*$  represents an *unknown (latent) group* whose membership is not annotated and therefore cannot be directly targeted by group-conditional objectives such as Group DRO.

For any  $G \subseteq \mathcal{X} \times \mathcal{Y}$ , define the subgroup risk

$$\mathcal{R}_G(h) = \mathbb{E}_{(x,y) \sim \mathcal{D}} [\ell(h(x), y) \mid (x, y) \in G].$$

where  $h : \mathcal{X} \rightarrow \mathcal{Y}$ .

**Definition 3.1** (Empirical Risk Minimization (ERM)). Empirical Risk Minimization selects a hypothesis

$$h_{\text{ERM}} \in \arg \min_{h \in \mathcal{H}} \mathcal{R}(h), \quad \mathcal{R}(h) = \mathbb{E}_{(x,y) \sim \mathcal{D}} [\ell(h(x), y)].$$

Equivalently, ERM minimizes a prevalence-weighted average of subgroup risks,

$$\mathcal{R}(h) = \sum_{G \in \mathcal{G}^*} \pi_G \mathcal{R}_G(h), \quad \pi_G = \mathbb{P}((x, y) \in G).$$

**Definition 3.2** (Group Distributionally Robust Optimization (Group DRO) (Sagawa et al., 2020)). Given access only to annotated groups  $\{G_1, \dots, G_K\}$ , Group DRO selects a hypothesis

$$h_{\text{DRO}} \in \arg \min_{h \in \mathcal{H}} \max_{G \in \{G_1, \dots, G_K\}} \mathcal{R}_G(h).$$

Although Group DRO provides worst-case guarantees over the annotated groups, it does not directly control performance on latent, unknown, subgroups that are present in the data but omitted from the optimization objective. Proposition 3.3 shows that worst-case optimization over known partitions can degrade performance on latent subpopulations relative to ERM when subgroup structure is incomplete. We use Group DRO as a seminal example, but this type of optimization for known groups extends to various other methods (Arjovsky & Bottou, 2017; Idrissi et al., 2021).

**Proposition 3.3.** *Let  $\mathcal{H}_{\text{DRO}}(\mathcal{G}') \subseteq \mathcal{H}$  (where  $\mathcal{G}' \subseteq \mathcal{G}$ ) denote the set of hypotheses that minimize the DRO objective over the known groups  $G \in \mathcal{G}'$ . Suppose we are given a latent partition  $\mathcal{G} = \{G_1, G_2, \dots, G_K\}$ . Then, we can always find  $i \in \{1, \dots, K\}$  such that at least one of the following is true about  $\mathcal{H}_{\text{DRO}}(\mathcal{G} \setminus \{G_i\})$*

- (i)  $h_{\text{ERM}} \in \mathcal{H}_{\text{DRO}}(\mathcal{G} \setminus \{G_i\})$
- (ii)  $\exists h \in \mathcal{H}_{\text{DRO}}(\mathcal{G} \setminus \{G_i\})$  s.t.  $\mathcal{R}_{G_i}(h) > \mathcal{R}_{G_i}(h_{\text{ERM}})$

*Proof sketch.* The argument hinges on comparing the Group DRO solution when all groups are known to the solution obtained when one group is omitted. Let  $h_{\text{DRO+}} \in \mathcal{H}_{\text{DRO}}(\mathcal{G})$  denote a minimizer of the Group DRO objective over all groups. There must exist a group  $G_i$  such that  $\mathcal{R}_{G_i}(h_{\text{DRO+}}) > \mathcal{R}_{G_i}(h_{\text{ERM}})$  in the nontrivial case that the hypotheses are not equal.

Fix the group  $G_i$  as unknown, and consider any minimizer  $h_{\text{DRO}} \in \mathcal{H}_{\text{DRO}}(\mathcal{G} \setminus \{G_i\})$ . Either  $h_{\text{DRO+}}$  is one such minimizer, for which we are done; otherwise, we must have  $\mathcal{R}_{G_i}(h_{\text{DRO}}) \geq \mathcal{R}_{G_i}(h_{\text{DRO+}})$ , otherwise we reach a contradiction with the definition of  $h_{\text{DRO+}}$ .  $\square$

We provide the full proof of the proposition in Appendix B.1. We also provide synthetic data results showing Proposition 3.3 in Appendix B.2.

## 4. Low-rank Error Informed Adaptation

The systematic failures on underrepresented subpopulations may manifest not as isolated mistakes, but as identifiable regions in representation space that are shared across many examples. Rather than correcting individual samples, a robust approach should directly identify and correct along directions in the representation space where errors are most concentrated. This intuition motivates **Low-rank Error Informed Adaptation (LEIA)**, which adopts a geometric perspective by viewing misclassification and uncertainty as arising from a low-dimensional structure in the learned representation space (Figure 2). By identifying principal directions along which high-loss examples concentrate, LEIA targets latent error modes without requiring subgroup labels (Algorithm 1).

**Stage 1 Training.** We consider a predictor that decomposes as  $m_\theta = c_\phi \circ e_\psi$  where  $e_\psi : \mathcal{X} \rightarrow \mathbb{R}^d$  is a feature extractor and  $c_\phi : \mathbb{R}^d \rightarrow \mathbb{R}^C$  is the classifier head. Given an input  $x$ , the model produces logits  $f(x) = c_\phi(e_\psi(x))$ . The training data is partitioned into two disjoint subsets:  $\mathcal{D}_{\text{ERM}}$  for base training and  $\mathcal{D}_{\text{LEIA}}$  for adaptation. We first train all parameters  $\theta = (\phi, \psi)$  on  $\mathcal{D}_{\text{ERM}}$  using standard empirical risk minimization (ERM), obtaining a checkpoint  $\hat{\theta} = (\hat{\phi}, \hat{\psi})$ . After convergence, both the feature extractor  $e_{\hat{\psi}}$  and the classifier head  $c_{\hat{\phi}}$  are frozen.

**Spectral Decomposition of Error-Weighted Covariance.** Using the frozen model  $m_{\hat{\theta}}$ , we compute logits  $f(x_i)$  for all  $(x_i, y_i) \in \mathcal{D}_{\text{LEIA}}$  and define example weights

$$\mu_i \propto \exp(\gamma \ell(f(x_i), y_i)), \quad \sum_i \mu_i = 1, \quad (1)$$

---

### Algorithm 1 Low-rank Error Informed Adaptation (LEIA)

---

**Input:**  $\mathcal{D}_{\text{ERM}}, \mathcal{D}_{\text{LEIA}}, k, \gamma$ , model  $m_\theta = c_\phi \circ e_\psi$

**Stage 1: ERM**

1. Train  $\theta = (\phi, \psi)$  on  $\mathcal{D}_{\text{ERM}}$  until convergence using ERM loss  $\mathcal{L}_{\text{ERM}}$

2. Freeze the feature extractor  $e_{\hat{\psi}}$

**Stage 2: Low-rank Error Informed Adaptation**

3. Compute example weights  $\mu_i$  from training losses (Equation 1).

4. Compute weighted feature covariance  $\Sigma_{\text{err}}$  and its top- $k$  eigenvectors  $V_k$  (Equation 2).

5. Learn a low-rank linear adjustment  $A$  restricted to  $\text{span}(V_k)$  via weighted risk minimization (Equation 4).

---

where  $\ell(\cdot)$  denotes cross-entropy loss and  $\gamma > 0$  determines the loss-weight sharpness. Let  $z_i = e_{\hat{\psi}}(x_i) \in \mathbb{R}^d$  and  $\bar{z} = \sum_i \mu_i z_i$ . We compute the error-weighted covariance

$$\Sigma_{\text{err}} = \sum_i \mu_i (z_i - \bar{z})(z_i - \bar{z})^\top \in \mathbb{R}^{d \times d}. \quad (2)$$

We retain the top- $k$  eigenvectors of  $\Sigma_{\text{err}}$ , forming  $V_k \in \mathbb{R}^{d \times k}$ , which defines a low-dimensional *error-informed subspace*.

**Low Rank Adjustment Learning.** Rather than retraining the full classifier, LEIA restricts adaptation to this error-informed subspace by low-rank additive correction directly in logit space. For input  $x$ , the adapted logits are

$$f_{\text{LEIA}}(x) = f(x) + A^\top V_k^\top e_{\hat{\psi}}(x), \quad (3)$$

where  $A \in \mathbb{R}^{k \times C}$  is the only learnable parameter. We optimize  $A$  by minimizing the weighted empirical risk

$$\min_A \sum_{(x_i, y_i) \in \mathcal{D}_{\text{LEIA}}} \mu_i \ell(f(x_i) + A^\top V_k^\top e_{\hat{\psi}}(x_i), y_i). \quad (4)$$

**Effect of Parameters.** LEIA introduces two hyperparameters: the rank  $k$  of the error-weighted subspace and the loss-weight sharpness  $\gamma$ . The rank  $k$  controls the expressivity of the correction, with smaller values yielding more structured updates and larger values capturing more complex error patterns; we select  $k$  in a data-driven manner based on the amount of error structure captured (Figure 2). The parameter  $\gamma$  controls how strongly high-loss examples are emphasized when forming the error-weighted covariance, with larger values focusing adaptation on the most uncertain or misclassified points. We tune both  $k$  and  $\gamma$  in our experiments.

## 5. Experiments

We evaluate LEIA on five benchmarks, compared against 12 baselines, and provide detailed ablations on design decisions and hyperparameters. Further details on datasets, baselines, and implementation can be found in Appendix C.

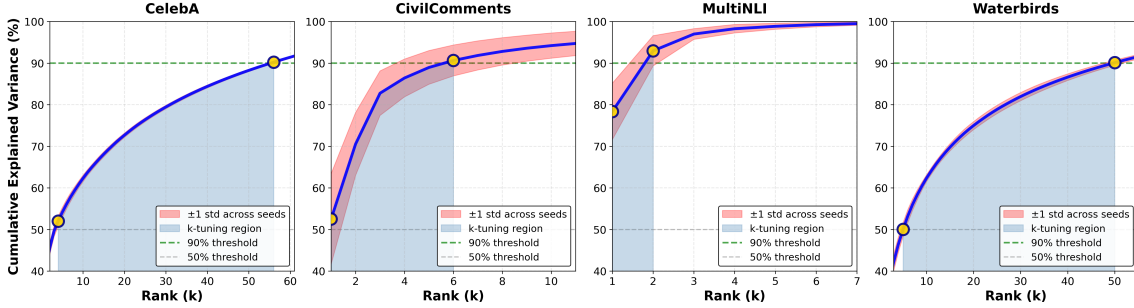


**Figure 2. Low-rank Error Structure across datasets.** The graphs show the cumulative explained variance (CEV) of the top- $k$  eigenvectors of the error-covariance matrix for (a) CELEBA; (b) CIVILCOMMENTS; (c) MULTINLI; and (d) WATERBIRDS. CEV is defined as  $\sum_{i=1}^k \lambda_i / \sum_{i=1}^n \lambda_i$ . The range of  $k$  for which the CEV is between 50% and 90% is shaded. The visualization demonstrates that (i) LEIA meaningfully learns an error-informed subspace; and (ii) this subspace is low-rank with respect to the embedding dimension (2048 for image datasets and 728 for text datasets).

### 5.1. Datasets

We consider five image and text classification benchmarks. Following (Qiu et al., 2023), we split the training set in a 80%–20% proportion for  $\mathcal{D}_{\text{ERM}}$  and  $\mathcal{D}_{\text{LEIA}}$ , but we show that performance is not very sensitive to the split in Appendix D.3.

**WATERBIRDS** (Sagawa et al., 2020) is an image classification dataset where bird types are associated with a spurious background attribute (water or land). **CELEBA** (Liu et al., 2015) is an image classification dataset, where hair color is an imbalanced attribute with respect to gender. **MULTINLI** (Williams et al., 2018) is a text benchmark of categorizing two sentences as entailing each other, contradicting each other, or neutral. The spurious correlation is between negation words like “never” and the “contradiction” label. **CIVILCOMMENTS** (Borkan et al., 2019) is a toxicity text classification dataset containing underrepresented demographic groups. **CHEXPERT** (Irvin et al., 2019) is a large-scale medical dataset of chest radiographs with rare pathologies, especially amongst certain minority groups.

### 5.2. Implementation

We follow standard model choices and dataset splits consistent with prior work (Liu et al., 2021; Kirichenko et al., 2022; Qiu et al., 2023): for Waterbirds, CelebA, and CheXpert, we use ResNet-50 (He et al., 2016) pretrained on ImageNet1k (Russakovsky et al., 2015), for MultiNLI and CivilComments we use BERT (Devlin et al., 2018) pre-trained on Book Corpus and English Wikipedia data.

LEIA’s hyperparameters  $k$  and  $\gamma$  are tuned on a held-out validation set. We choose  $k$  in a principled manner according to cumulative variance captured (see Figure 2).

### 5.3. Attribute Availability

We consider three settings of attribute availability:

- First, we consider the setting of *truly no information of subgroup relevance*. In many real-world scenarios, attribute annotations are not available during training or validation. In this setting, we apply hyperparameter selection and early stopping using the worst class label accuracy (Yang et al., 2023; To et al., 2025).
- Next, we study the unique setting of *partial knowledge of subgroup relevance*. Here, we have only some subgroups defined during training and validation, and then assess performance on the entire set of subgroups, which includes unknown subgroups. This setting simulates scenarios where all spurious features or sensitive attributes may **not** be known during training. From this setting, we assess worst group performance on latent subgroups and whether methods overfit performance to known subgroups. We apply hyperparameter selection and early stopping using the worst group accuracy (WGA) over the set of known groups.
- Finally, to compare with recent works (Kirichenko et al., 2022; Qiu et al., 2023; To et al., 2025), we consider a scenario where there is *complete knowledge of subgroup relevance* with the assumption that all subgroups of interest are well-defined and available in the validation set. We stress that this setting is not realistic but provided to compare with previous results. In this setting, we apply hyperparameter selection and early stopping using the WGA over all subgroups.

### 5.4. Baselines

To rigorously evaluate the effectiveness of LEIA, we compare performance against current state-of-the-art methods: Classifier Re-train (**CRT**, **ReweightCRT**) (Kang et al., 2020), Just Train Twice (**JTT**) (Liu et al., 2021), (**CVaRDRO**) (Duchi & Namkoong, 2020), Deep Feature Reweighting (**DFR**) (Kirichenko et al., 2022), Learning Invariant Predictors with Selective Augmentation (**LISA**) (Yao et al., 2022), Correct-n-Contrast (**CnC**) (Zhang et al., 2022), Automatic Feature Reweighting (**AFR**) (Qiu et al.,

**Table 1. Worst-group accuracy (WGA) and average accuracy on the test set with no information of group relevance.** Rows with asterisks (\*) reproduces baselines. Other results are reported from original papers of competitive baselines. Group Info (Train/Val) indicates whether group labels are used:  $\times$  = no group info used. Best and second-best values are **bold** and underlined, respectively. “-” indicates results not reported. All results are the mean  $\pm$  standard deviation (in %) averaged over three independent runs.

Algorithm	Group Info (Train/Val)	WATERBIRDS		CELEBA		CIVILCOMMENTS		MULTINLI		CHEXPERT	
		WGA	Avg Acc								
ERM*	$\times/\times$	69.1 $\pm$ 4.7	84.1 $\pm$ 1.7	57.6 $\pm$ 0.8	95.0 $\pm$ 0.1	63.2 $\pm$ 1.2	<u>85.4</u> $\pm$ 0.2	66.4 $\pm$ 2.3	81.0 $\pm$ 0.3	41.7 $\pm$ 3.4	<b>88.6</b> $\pm$ 0.7
CRT*	$\times/\times$	76.3 $\pm$ 0.8	89.2 $\pm$ 0.1	69.6 $\pm$ 0.7	94.1 $\pm$ 0.1	67.8 $\pm$ 0.3	82.7 $\pm$ 0.1	65.4 $\pm$ 0.2	80.2 $\pm$ 0.0	74.6 $\pm$ 0.4	79.3 $\pm$ 0.1
ReWeightCRT*	$\times/\times$	76.3 $\pm$ 0.2	89.4 $\pm$ 0.3	70.7 $\pm$ 0.6	94.2 $\pm$ 0.1	64.7 $\pm$ 0.2	82.4 $\pm$ 0.0	65.2 $\pm$ 0.2	80.2 $\pm$ 0.0	75.1 $\pm$ 0.2	79.3 $\pm$ 0.1
JTT*	$\times/\times$	71.2 $\pm$ 0.5	88.9 $\pm$ 0.6	48.3 $\pm$ 1.5	<b>95.9</b> $\pm$ 0.0	51.0 $\pm$ 4.2	79.0 $\pm$ 1.8	65.1 $\pm$ 1.6	<u>81.4</u> $\pm$ 0.0	60.4 $\pm$ 4.8	75.2 $\pm$ 0.8
CVaRDRO*	$\times/\times$	75.5 $\pm$ 2.2	89.9 $\pm$ 0.4	60.2 $\pm$ 3.0	95.1 $\pm$ 0.1	62.9 $\pm$ 3.8	81.6 $\pm$ 0.7	48.2 $\pm$ 3.4	75.4 $\pm$ 0.2	50.2 $\pm$ 1.8	73.7 $\pm$ 1.0
DFR*	$\times/\times$	89.0 $\pm$ 0.2	92.2 $\pm$ 0.2	73.7 $\pm$ 0.8	93.6 $\pm$ 0.0	64.4 $\pm$ 0.1	80.7 $\pm$ 0.0	63.8 $\pm$ 0.0	80.2 $\pm$ 0.0	<b>75.8</b> $\pm$ 0.3	79.1 $\pm$ 0.0
DPE	$\times/\times$	<b>91.0</b> $\pm$ 0.5	<u>92.5</u> $\pm$ 0.2	<u>81.9</u> $\pm$ 0.2	89.8 $\pm$ 0.2	<u>69.9</u> $\pm$ 0.9	82.2 $\pm$ 0.2	<u>69.3</u> $\pm$ 0.8	81.3 $\pm$ 0.2	—	—
LISA*	$\times/\times$	77.5 $\pm$ 0.7	89.2 $\pm$ 0.6	57.8 $\pm$ 0.8	<u>95.4</u> $\pm$ 0.1	65.8 $\pm$ 1.5	84.6 $\pm$ 0.1	66.8 $\pm$ 0.3	<b>81.7</b> $\pm$ 0.1	37.4 $\pm$ 3.5	<u>81.9</u> $\pm$ 6.2
LEIA (Ours)	$\times/\times$	<u>90.1</u> $\pm$ 0.1	<b>93.7</b> $\pm$ 0.7	<b>82.8</b> $\pm$ 0.5	95.2 $\pm$ 0.1	<b>71.6</b> $\pm$ 0.7	<b>91.4</b> $\pm$ 0.4	<b>69.7</b> $\pm$ 0.1	81.2 $\pm$ 0.2	75.3 $\pm$ 0.4	79.6 $\pm$ 0.2

2023), Group Inference via data Comparison (**GIC**) (Han & Zou, 2024), and Diverse Prototypical Ensembles (**DPE**) (To et al., 2025). We also compare performance with **ERM** and **Group DRO** (Sagawa et al., 2020).

## 6. Results

### 6.1. LEIA Achieves Strong Group Robustness

**No Information of Group Relevance.** In the setting with no attribute information known in training or validation, our method LEIA achieves best or second best worst group accuracy (WGA) in *all* datasets (see Table 1). In particular, we show excellent performance on the **CIVILCOMMENTS** dataset where we achieve both the highest WGA at a 1.7% increase to the second highest baseline (DPE) and a 6.0% average accuracy increase from standard training (ERM). For the **CELEBA** dataset, we achieve the highest WGA with an impressive average accuracy of 95.2%. The closest baseline that exhibits such a high average accuracy is LISA, with a WGA  $\sim$ 24.0% lower.

**Partial Information of Group Relevance.** In Section 3, we highlight the importance of considering unknown groups, as in many real-world scenarios, relevant subgroups will not be known *a priori*. We create a training and evaluation setup with the **CIVILCOMMENTS** and **CHEXPERT** datasets.

The **CIVILCOMMENTS** dataset contains binary toxicity labels  $y \in \{0, 1\}$  and annotations for eight demographic attributes  $\mathcal{A} = \{\text{male, female, LGBTQ, Christian, Muslim, other religion, Black, White}\}$ . In our case study setup, all methods are trained on the full training data. However, we define subgroups using only a *single* attribute  $a \in \mathcal{A}$ . Specifically, we construct four training groups based on the cross-product of toxicity and the selected attribute:  $g \in \mathcal{G}_{\text{train}}(a) = \{\text{non-toxic no } a; \text{ non-toxic has } a; \text{ toxic no } a; \text{ toxic has } a\}$ . All methods use only these four known groups for training and validation. At evaluation

time, we assess performance across all demographic attributes. Concretely, we evaluate on the 16 test groups  $\mathcal{G}_{\text{test}} = \{(y, a_j) \mid y \in \{0, 1\}, a_j \in \mathcal{A}\}$ . Groups with  $a_j \neq a$  are *unknown subgroups*. We focus on Black, LGBTQ, and Muslim as the known training attributes, as they are realistic in toxic content moderation and exhibit poor worst-group performance under ERM (Duchene et al., 2023).

The **CHEXPERT** dataset contains binary labels  $y \in \{0, 1\}$  indicating the presence of a medical condition, with race  $\in \{\text{White, Black, Other}\}$  and gender  $\in \{\text{Male, Female}\}$ . As above, all methods are trained on the full dataset, but subgroups are defined using only one demographic attribute at a time. We consider: (i) *Race-only* training with  $\mathcal{G}_{\text{train}}(\text{race}) = \{y \times \text{race}\}$  and (ii) *Gender-only* training with  $\mathcal{G}_{\text{train}}(\text{gender}) = \{y \times \text{gender}\}$ . Only the corresponding known groups are used for training and validation. Evaluation is performed over the full intersection,  $\mathcal{G}_{\text{test}} = \{(y, \text{race, gender})\}$ , yielding 12 test groups. Groups involving the attribute not used during training are *unknown subgroups*. For example, in race-only training, worst-group performance is computed over all race  $\times$  gender  $\times$  label groups. These settings reflect realistic scenarios where only partial demographic information is available during training, while deployment requires robustness across full demographic intersections.

In Table 2, we show that LEIA has the best WGA across all groups in four out of five settings. On average, LEIA has a 1.1%-2.4% increase in WGA from the second highest baseline. We also observe that LEIA has far more stable performance with lower standard deviations than other baselines, especially with the **CHEXPERT** results. Notably, we observe how competitive baselines like AFR, DFR, and GroupDRO, perform considerably worse than in the setting with complete information of group relevance.

**Table 2. Worst-group accuracy (WGA) and average accuracy on the test set under partial information of group relevance.** For CHEXPERT, known groups are defined by race or gender, while WGA is computed over all race  $\times$  gender groups. For CIVILCOMMENTS, training uses four groups defined by a single known attribute (Black, LGBTQ, or Muslim), and WGA is evaluated over all 16 demographic groups. Group Info (Train/Val) denotes group-label usage:  $\times$  = none,  $\checkmark$  = training,  $\checkmark\checkmark$  = validation labels used to retrain,  $\star$  = validation labels for tuning/early stopping only. Best and second-best results are **bold** and underlined. All results are the mean  $\pm$  std. (in %) over five independent runs.

Algorithm	Group Info		CHEXPERT				CIVILCOMMENTS					
	Known Attribute	(Train/Val)	Race		Gender		Black		LGBTQ		Muslim	
			WGA	Avg Acc								
ERM	$\times/\star$		41.7 $\pm$ 3.4	88.6 $\pm$ 0.7	41.7 $\pm$ 3.4	88.6 $\pm$ 0.7	48.0 $\pm$ 7.5	<b>92.3</b> $\pm$ 0.1	48.0 $\pm$ 7.5	<b>92.3</b> $\pm$ 0.1	48.0 $\pm$ 7.5	<b>92.3</b> $\pm$ 0.1
CRT	$\times/\star$		71.1 $\pm$ 6.9	80.9 $\pm$ 1.7	71.2 $\pm$ 6.9	80.8 $\pm$ 1.8	62.8 $\pm$ 3.5	90.4 $\pm$ 1.9	63.1 $\pm$ 3.5	90.6 $\pm$ 1.6	61.5 $\pm$ 2.5	90.0 $\pm$ 2.2
ReWeightCRT	$\times/\star$		71.3 $\pm$ 6.1	80.8 $\pm$ 1.9	71.3 $\pm$ 6.1	80.7 $\pm$ 1.9	61.9 $\pm$ 3.2	90.7 $\pm$ 1.6	63.4 $\pm$ 3.5	90.7 $\pm$ 1.3	62.1 $\pm$ 2.3	90.4 $\pm$ 1.7
JTT	$\times/\star$		58.7 $\pm$ 15.0	84.5 $\pm$ 4.0	58.7 $\pm$ 15.0	84.5 $\pm$ 4.0	57.8 $\pm$ 2.4	91.9 $\pm$ 0.2	57.7 $\pm$ 2.5	91.9 $\pm$ 0.2	57.6 $\pm$ 2.7	91.9 $\pm$ 0.2
CVaRDRO	$\times/\star$		37.1 $\pm$ 17.6	88.0 $\pm$ 4.2	37.1 $\pm$ 17.6	88.0 $\pm$ 4.2	57.1 $\pm$ 3.1	91.9 $\pm$ 0.2	55.8 $\pm$ 3.2	92.1 $\pm$ 0.3	56.2 $\pm$ 2.8	<b>92.0</b> $\pm$ 0.2
AFR	$\times/\star$		63.9 $\pm$ 13.1	82.9 $\pm$ 3.7	63.9 $\pm$ 13.1	82.9 $\pm$ 3.7	38.1 $\pm$ 11.8	<b>92.0</b> $\pm$ 0.7	38.4 $\pm$ 11.7	<b>92.0</b> $\pm$ 0.7	38.2 $\pm$ 11.8	92.0 $\pm$ 0.7
DFR	$\times/\checkmark\checkmark$		63.9 $\pm$ 10.6	72.3 $\pm$ 6.0	63.4 $\pm$ 11.5	72.3 $\pm$ 6.0	66.5 $\pm$ 2.6	90.6 $\pm$ 0.6	64.0 $\pm$ 1.6	90.1 $\pm$ 1.6	<b>64.1</b> $\pm$ 4.5	89.2 $\pm$ 1.1
Group DRO	$\checkmark/\star$		69.6 $\pm$ 7.6	80.9 $\pm$ 1.9	70.0 $\pm$ 7.5	80.9 $\pm$ 1.9	66.7 $\pm$ 1.9	89.5 $\pm$ 2.3	62.9 $\pm$ 4.0	89.3 $\pm$ 2.5	63.3 $\pm$ 3.4	89.4 $\pm$ 2.3
IRM	$\checkmark/\star$		71.4 $\pm$ 7.2	81.0 $\pm$ 1.7	71.3 $\pm$ 7.0	80.9 $\pm$ 1.8	<b>67.0</b> $\pm$ 1.6	90.0 $\pm$ 1.4	64.4 $\pm$ 1.6	90.3 $\pm$ 1.5	63.6 $\pm$ 3.2	89.3 $\pm$ 1.5
LISA	$\checkmark/\star$		39.5 $\pm$ 2.7	<b>89.4</b> $\pm$ 0.5	44.7 $\pm$ 3.1	<b>88.7</b> $\pm$ 0.4	61.7 $\pm$ 5.7	91.3 $\pm$ 0.7	59.2 $\pm$ 2.5	91.7 $\pm$ 0.2	59.4 $\pm$ 5.1	91.6 $\pm$ 0.6
LEIA (Ours)	$\times/\star$		<b>73.4</b> $\pm$ 1.9	78.7 $\pm$ 0.8	<b>73.3</b> $\pm$ 1.7	78.5 $\pm$ 1.2	66.1 $\pm$ 1.2	90.2 $\pm$ 0.7	<b>66.8</b> $\pm$ 1.9	90.1 $\pm$ 0.7	<b>65.2</b> $\pm$ 1.8	89.5 $\pm$ 0.4

**Table 3. Worst-group accuracy (WGA) and average accuracy on the test set with complete information of group relevance.** Baselines are divided into two types based on whether group labels are required for training the method. Rows denoted with asterisks (\*) and CheXpert results reproduces baselines. Other results are reported from original papers of competitive baselines. Group Info (Train/Val) indicates whether group labels are used:  $\times$  = no group info used,  $\star$  = group info used for hyperparameter tuning and early stopping. Best and second-best values within each half are **bold** and underlined, respectively. “-” indicates results not reported. All of our results are the mean  $\pm$  standard deviation (in %) averaged over three independent runs.

Algorithm	Group Info		WATERBIRDS		CELEBA		CIVILCOMMENTS		MULTINLI		CHEXPERT		
	(Train/Val)	WGA	Avg Acc	WGA	Avg Acc	WGA	Avg Acc	WGA	Avg Acc	WGA	Avg Acc	WGA	Avg Acc
ERM*	$\times/\star$	69.1 $\pm$ 4.7	84.1 $\pm$ 1.7	57.6 $\pm$ 0.8	<u>95.0</u> $\pm$ 0.1	63.2 $\pm$ 1.2	85.4 $\pm$ 0.2	69.5 $\pm$ 0.3	80.9 $\pm$ 0.3	41.7 $\pm$ 3.4	<b>88.6</b> $\pm$ 0.7		
CRT*	$\times/\star$	76.3 $\pm$ 0.8	89.2 $\pm$ 0.1	70.4 $\pm$ 0.4	94.1 $\pm$ 0.1	68.5 $\pm$ 0.0	83.0 $\pm$ 0.0	65.4 $\pm$ 0.1	80.2 $\pm$ 0.0	74.0 $\pm$ 0.2	79.1 $\pm$ 0.1		
ReWeightCRT*	$\times/\star$	76.3 $\pm$ 0.2	89.4 $\pm$ 0.3	71.1 $\pm$ 0.5	94.2 $\pm$ 0.1	68.2 $\pm$ 0.4	83.4 $\pm$ 0.0	65.3 $\pm$ 0.1	80.2 $\pm$ 0.0	73.9 $\pm$ 0.2	79.0 $\pm$ 0.1		
JTT	$\times/\star$	86.7	93.3	81.1	88.0	69.3	<b>91.1</b>	<u>72.6</u>	78.6	60.4 $\pm$ 4.8	75.2 $\pm$ 0.8		
CVaRDRO*	$\times/\star$	75.5 $\pm$ 2.2	89.9 $\pm$ 0.4	62.2 $\pm$ 3.1	95.1 $\pm$ 0.1	68.7 $\pm$ 1.3	83.5 $\pm$ 0.3	63.0 $\pm$ 1.5	75.1 $\pm$ 0.1	50.2 $\pm$ 1.8	73.7 $\pm$ 1.0		
CnC	$\times/\star$	88.5 $\pm$ 0.3	90.9 $\pm$ 0.1	<u>88.8</u> $\pm$ 0.9	89.9 $\pm$ 0.5	68.9 $\pm$ 2.1	81.7 $\pm$ 0.5	—	—	—	—		
AFR	$\times/\star$	90.4 $\pm$ 1.1	<b>94.2</b> $\pm$ 1.2	82.0 $\pm$ 0.5	91.3 $\pm$ 0.3	68.7 $\pm$ 0.6	89.8 $\pm$ 0.6	<b>73.4</b> $\pm$ 0.6	<u>81.4</u> $\pm$ 0.2	—	—		
GIC	$\times/\star$	86.3 $\pm$ 0.1	89.6 $\pm$ 1.3	<b>89.4</b> $\pm$ 0.2	91.9 $\pm$ 0.1	72.5 $\pm$ 0.3	90.0 $\pm$ 0.3	—	—	—	—		
LEIA (Ours)	$\times/\star$	<b>90.7</b> $\pm$ 0.2	<u>93.3</u> $\pm$ 0.7	85.0 $\pm$ 0.9	<b>95.2</b> $\pm$ 0.1	<b>72.9</b> $\pm$ 0.2	90.9 $\pm$ 0.8	69.6 $\pm$ 0.8	<b>81.4</b> $\pm$ 0.4	<b>75.2</b> $\pm$ 0.3	79.6 $\pm$ 0.3		

**Complete Information of Group Relevance.** As this is the typical setting used for assessing performance of algorithms that do not use group information for training, we show that LEIA’s performance remains strong when comparing against state-of-the-art baselines (see Table 11). LEIA achieves the highest WGA on WATERBIRDS, CIVILCOMMENTS, and CHEXPERT datasets in this setting where we use validation WGA for hyperparameter tuning and early stopping. Again, we observe impressive subgroup performance without significant trade-offs to average performance. In the CELEBA dataset, we achieve 85.0% WGA while maintaining 95.2% average accuracy. While CnC and GIC outperform LEIA in WGA by 3.8-4.4%, this comes at a drop in overall accuracy of 3.3%-5.3%.

We note that if oracle group labels are fully available, one would use Group DRO or other methods that train with these

oracle labels, as they outperform methods that do not use group labels for training (see Appendix D.1 for results). We emphasize that such oracle knowledge of group relevancy is unrealistic. But in assessing performance with comparable baselines, LEIA exhibits strong performance. LEIA’s performance in all three settings is even more impressive given how lightweight and fast it is compared to baselines.

## 6.2. LEIA is Fast and Parameter-Efficient

In Figure 3, we visualize the training time required by LEIA and baselines on four datasets, as other state-of-the-art baselines have not shown results on CheXpert. LEIA has a 10.8% average overhead compared to ERM, with AFR following at a 11.7% overhead. Other baselines are heavier: DPE has a 71.6% overhead; JTT has a 203.1% overhead; GIC has a 407.9% overhead. We also provide details and a

table in Appendix C.4 for readability.

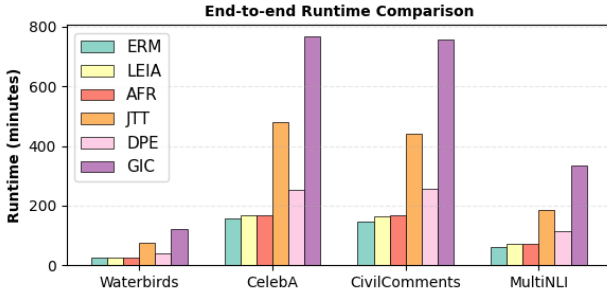


Figure 3. **Training time** (in minutes) across different datasets. LEIA only incurs a small overhead compared to standard ERM and is substantially less expensive than recent methods like JTT, DPE, and GIC.

Table 4 highlights that LEIA is a particularly attractive in settings where computational budget, memory, or training stability are key constraints. Unlike competing methods that update parameters proportional to the embedding dimension or even the full backbone, LEIA updates only a low-rank set of class-specific parameters, scaling as  $k \times C$ .

Table 4. **Number of trainable parameters** updated during the second stage training for comparative baselines.  $k$  = LEIA rank parameter,  $d$  = embedding dimension,  $C$  = number of classes,  $N$  = DPE number of prototypes per class, and  $P_{\text{backbone}}$  = total parameters of base model backbone. For LEIA, we include the *maximum* number of parameters updated across all runs, since the  $k$  parameter is tuned for each seed.

Algorithm	WATERBIRDS	CELEBA	CIVILCOMMENTS	MULTINLI
LEIA ( $k \times C$ )	32	104	18	9
AFR ( $d \times C$ )	4,098	4,098	1,456	2,184
DPE ( $N \times d \times C$ )	61,470	61,470	21,840	32,760
JTT ( $P_{\text{backbone}}$ )	23,512,130	23,512,130	109,483,778	109,483,778
GIC ( $2 \times P_{\text{backbone}}$ )	47,024,260	47,024,260	218,967,556	218,967,556

### 6.3. LEIA is Robust to Hyperparameters

We study the robustness of LEIA to the choice of the hyperparameter  $k$ . Furthermore in Appendix D, we present additional results of ablating the  $\gamma$  parameter and dataset splitting ratios.

We find that throughout the range of  $k$  values highlighted in Figure 2, LEIA achieves competitive WGA performance across datasets. For WATERBIRDS and CIVILCOMMENTS datasets, we can see that there is more variance in lower ranks, suggesting that there is not enough cumulative variance captured with the lower error directions across all seeds, leading to less consistent performance (see Figure 4) However, as performance stabilizes, variation is limited to less than 1% across ranks. The  $\gamma$  parameter shows similar robustness (see Figure 7). Taken together, the rank and  $\gamma$  robustness analyses show that LEIA has two relatively forgiving hyperparameters, making it substantially easier to use than methods that require precise hyperparameter tuning.

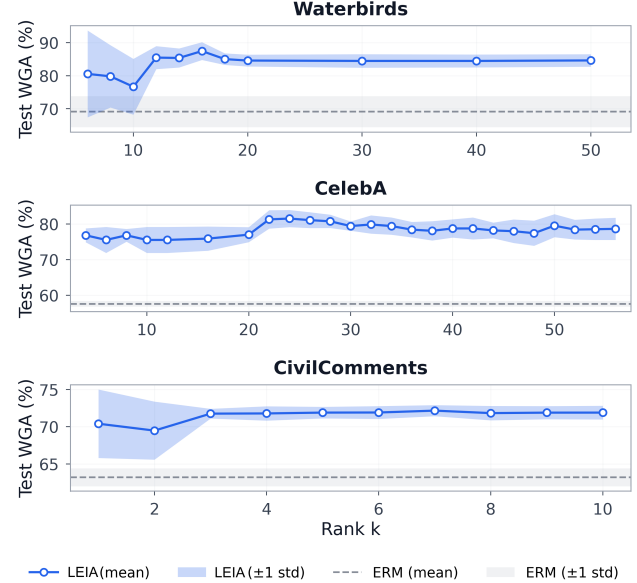


Figure 4. **Robustness of LEIA to rank  $k$  parameter:** We show how LEIA has strong test WGA performance throughout the  $k$  tuning region identified in Figure 2. Performance is averaged across 3 seeds.

## 7. Conclusion

We study the realistic setting of group robustness when subpopulations are unknown at training time and show that robustness guarantees over known groups do not hold on unknown subpopulations. We propose *Low-rank Error Informed Adaptation (LEIA)*, a simple two-stage method that identifies low-dimensional subspace in the representation space where model errors concentrate and restricts adaptation to this error-informed subspace via a low-rank adjustment to the classifier logits. Across five benchmarks, LEIA consistently improves worst-group performance under (1) truly no knowledge of subgroup relevance, (2) partial knowledge of subgroup relevance, and (3) full knowledge of subgroup relevance. Beyond empirical gains, our results show that evaluating robustness methods solely under full subgroup knowledge substantially overestimates real-world reliability. Thus, we call for *partial knowledge of subgroup relevancy to be treated as a first-class evaluation regime* in group robustness research.

## Impact Statement

This work introduces Low-rank Error Informed Adaptation (LEIA), a method that furthers the efficiency frontier of group robustness methods and improves group robustness in settings where subpopulations most affected by model failures are unlabeled, unknown, or only partially observed at training time. LEIA aims to mitigate systematic failures arising from the effects of subpopulation shift through a low-rank error correction term, all without requiring ex-

plicit subgroup annotations. As machine learning models are deployed in high-stakes scenarios for heterogeneous populations, it is critical that models are performant across subgroups. The particular societal impact of our work is the consideration of realistic deployment scenarios where group attributes are not fully available to train models and oracle knowledge of relevant subgroups is not present. While LEIA shows impressive performance across experiments, it does not eliminate all biases inherent in data or model architectures. Further research is necessary to assess LEIA’s effectiveness across diverse datasets, out of distribution settings, and real-world model pipelines.

## References

Ahmed, F., Bengio, Y., van Seijen, H., and Courville, A. Systematic generalisation with group invariant predictions. In *International Conference on Learning Representations*, 2021. URL <https://openreview.net/forum?id=b9PoimzFJ>.

Arjovsky, M. and Bottou, L. Towards principled methods for training generative adversarial networks, 2017. URL <https://arxiv.org/abs/1701.04862>.

Arjovsky, M., Bottou, L., Gulrajani, I., and Lopez-Paz, D. Invariant risk minimization. *arXiv preprint arXiv:1907.02893*, 2019.

Awasthi, P., Kleindessner, M., and Morgenstern, J. Equalized odds postprocessing under imperfect group information. In Chiappa, S. and Calandra, R. (eds.), *Proceedings of the Twenty Third International Conference on Artificial Intelligence and Statistics*, volume 108 of *Proceedings of Machine Learning Research*, pp. 1770–1780. PMLR, 26–28 Aug 2020. URL <https://proceedings.mlr.press/v108/awasthi20a.html>.

Balashankar, A., Lees, A., Welty, C., and Subramanian, L. What is fair? exploring pareto-efficiency for fairness constrained classifiers. *arXiv preprint arXiv:1910.14120*, 2019.

Banerjee, I., Bhattacharjee, K., Burns, J. L., Trivedi, H., Purkayastha, S., Seyyed-Kalantari, L., Patel, B. N., Shridhar, R., and Gichoya, J. “shortcuts” causing bias in radiology artificial intelligence: causes, evaluation, and mitigation. *Journal of the American College of Radiology*, 20(9):842–851, 2023.

Beery, S., Van Horn, G., and Perona, P. Recognition in terra incognita. In *Proceedings of the European conference on computer vision (ECCV)*, pp. 456–473, 2018.

Borkan, D., Dixon, L., Sorensen, J., Thain, N., and Vasserman, L. Nuanced Metrics For Measuring Unintended Bias With Real Data For Text Classification. *Companion proceedings of the 2019 world wide web conference*, pp. 491–500, 2019.

Buolamwini, J. and Gebru, T. Gender shades: Intersectional accuracy disparities in commercial gender classification. In Friedler, S. A. and Wilson, C. (eds.), *Proceedings of the 1st Conference on Fairness, Accountability and Transparency*, volume 81 of *Proceedings of Machine Learning Research*, pp. 77–91. PMLR, 23–24 Feb 2018. URL <https://proceedings.mlr.press/v81/buolamwini18a.html>.

Chuang, C.-Y., Jampani, V., Li, Y., Torralba, A., and Jegelka, S. Debiasing vision-language models via biased prompts. *arXiv preprint arXiv:2302.00070*, 2023.

Creager, E., Jacobsen, J.-H., and Zemel, R. Environment inference for invariant learning. In *International Conference on Machine Learning*, pp. 2189–2200. PMLR, 2021.

Devlin, J., Chang, M.-W., Lee, K., and Toutanova, K. BERT: Pre-training Of Deep Bidirectional Transformers For Language Understanding. *arXiv preprint arXiv:1810.04805*, 2018.

Du, Y., Yan, J., Chen, Y., Liu, J., Zhao, S., She, Q., Wu, H., Wang, H., and Qin, B. Less learn shortcut: Analyzing and mitigating learning of spurious feature-label correlation, 2023. URL <https://arxiv.org/abs/2205.12593>.

Duchene, C., Jamet, H., Guillaume, P., and Dehak, R. A benchmark for toxic comment classification on civil comments dataset, 2023. URL <https://arxiv.org/abs/2301.11125>.

Duchi, J. and Namkoong, H. Learning models with uniform performance via distributionally robust optimization, 2020. URL <https://arxiv.org/abs/1810.08750>.

Geirhos, R., Jacobsen, J.-H., Michaelis, C., Zemel, R., Brendel, W., Bethge, M., and Wichmann, F. A. Shortcut Learning In Deep Neural Networks. *Nature Machine Intelligence*, 2(11):665–673, 2020.

Gerych, W., Zhang, H., Hamidieh, K., Pan, E., Sharma, M. K., Hartvigsen, T., and Ghassemi, M. Bendvlm: Test-time debiasing of vision-language embeddings. *Advances in Neural Information Processing Systems*, 37:62480–62502, 2024.

Goel, K., Gu, A., Li, Y., and Ré, C. Model patching: Closing the subgroup performance gap with data augmentation. *arXiv preprint arXiv:2008.06775*, 2020.

Han, Y. and Zou, D. Improving group robustness on spurious correlation requires preciser group inference, 2024. URL <https://arxiv.org/abs/2404.13815>.

Hashimoto, T., Srivastava, M., Namkoong, H., and Liang, P. Fairness without demographics in repeated loss minimization. In *International Conference on Machine Learning*, pp. 1929–1938. PMLR, 2018.

He, K., Zhang, X., Ren, S., and Sun, J. Deep Residual Learning For Image Recognition. *Proceedings of the IEEE conference on computer vision and pattern recognition*, pp. 770–778, 2016.

Hirota, Y., Chen, M.-H., Wang, C.-Y., Nakashima, Y., Wang, Y.-C. F., and Hachiuma, R. Saner: Annotation-free societal attribute neutralizer for debiasing clip. *arXiv preprint arXiv:2408.10202*, 2024.

Hu, E. J., Shen, Y., Wallis, P., Allen-Zhu, Z., Li, Y., Wang, S., Wang, L., Chen, W., et al. Lora: Low-rank adaptation of large language models. *ICLR*, 1(2):3, 2022.

Idrissi, B. Y., Arjovsky, M., Pezeshki, M., and Lopez-Paz, D. Simple Data Balancing Achieves Competitive Worst-Group-Accuracy. *arXiv preprint arXiv:2110.14503*, 2021.

Irvin, J., Rajpurkar, P., Ko, M., Yu, Y., Ciurea-Ilcus, S., Chute, C., Marklund, H., Haghgoo, B., Ball, R., Shpanskaya, K., Seekins, J., Mong, D. A., Halabi, S. S., Sandberg, J. K., Jones, R., Larson, D. B., Langlotz, C. P., Patel, B. N., Lungren, M. P., and Ng, A. Y. Chexpert: A large chest radiograph dataset with uncertainty labels and expert comparison, 2019. URL <https://arxiv.org/abs/1901.07031>.

Jain, S., Hamidieh, K., Georgiev, K., Ilyas, A., Ghassemi, M., and Madry, A. Improving subgroup robustness via data selection. *Advances in Neural Information Processing Systems*, 37:94490–94511, 2024.

Jang, T., Jung, H., and Wang, X. Target bias is all you need: Zero-shot debiasing of vision-language models with bias corpus. In *Proceedings of the IEEE/CVF International Conference on Computer Vision*, pp. 1935–1946, 2025.

Japkowicz, N. The class imbalance problem: Significance and strategies. In *Proc. of the Int'l Conf. on artificial intelligence*, volume 56, pp. 111–117, 2000.

Jung, H., Jang, T., and Wang, X. A unified debiasing approach for vision-language models across modalities and tasks. *Advances in Neural Information Processing Systems*, 37:21034–21058, 2024.

Kallus, N., Mao, X., and Zhou, A. Assessing algorithmic fairness with unobserved protected class using data combination. *Management Science*, 68(3):1959–1981, 2022.

Kang, B., Xie, S., Rohrbach, M., Yan, Z., Gordo, A., Feng, J., and Kalantidis, Y. Decoupling representation and classifier for long-tailed recognition, 2020. URL <https://arxiv.org/abs/1910.09217>.

Kaplow, L. and Shavell, S. The conflict between notions of fairness and the pareto principle. *American Law and Economics Review*, 1(1):63–77, 1999.

Kearns, M., Neel, S., Roth, A., and Wu, Z. S. Preventing fairness gerrymandering: Auditing and learning for subgroup fairness. In Dy, J. and Krause, A. (eds.), *Proceedings of the 35th International Conference on Machine Learning*, volume 80 of *Proceedings of Machine Learning Research*, pp. 2564–2572. PMLR, 10–15 Jul 2018. URL <https://proceedings.mlr.press/v80/kearns18a.html>.

Kirichenko, P., Izmailov, P., and Wilson, A. G. Last Layer Re-Training Is Sufficient For Robustness To Spurious Correlations. *Preprint arXiv 2204.02937v1*, 2022.

Kleinberg, J., Ludwig, J., Mullainathan, S., and Ramabachan, A. Algorithmic fairness. *AEA Papers and Proceedings*, 108:22–27, May 2018. doi: 10.1257/pandp.20181018. URL <https://www.aeaweb.org/articles?id=10.1257/pandp.20181018>.

Koh, P. W., Sagawa, S., Marklund, H., Xie, S. M., Zhang, M., Balsubramani, A., Hu, W., Yasunaga, M., Phillips, R. L., Gao, I., Lee, T., David, E., Stavness, I., Guo, W., Earnshaw, B. A., Haque, I. S., Beery, S., Leskovec, J., Kundaje, A., Pierson, E., Levine, S., Finn, C., and Liang, P. Wilds: A benchmark of in-the-wild distribution shifts, 2021. URL <https://arxiv.org/abs/2012.07421>.

Krumpal, I. Determinants of social desirability bias in sensitive surveys: a literature review. *Quality & quantity*, 47(4):2025–2047, 2013.

LaBonte, T., Muthukumar, V., and Kumar, A. Towards last-layer retraining for group robustness with fewer annotations. *Advances in Neural Information Processing Systems*, 36:11552–11579, 2023.

Lahoti, P., Beutel, A., Chen, J., Lee, K., Prost, F., Thain, N., Wang, X., and Chi, E. Fairness without demographics through adversarially reweighted learning. *Advances in neural information processing systems*, 33:728–740, 2020.

Liu, E. Z., Haghgoo, B., Chen, A. S., Raghunathan, A., Koh, P. W., Sagawa, S., Liang, P., and Finn, C. Just Train Twice: Improving Group Robustness Without Training Group Information. *International Conference on Machine Learning (ICML)*, 2021.

Liu, Z., Luo, P., Wang, X., and Tang, X. Deep learning face attributes in the wild. In *2015 IEEE International Conference on Computer Vision (ICCV)*, pp. 3730–3738, 2015. doi: 10.1109/ICCV.2015.425.

Liu, Z., Miao, Z., Zhan, X., Wang, J., Gong, B., and Yu, S. X. Large-scale long-tailed recognition in an open world, 2019. URL <https://arxiv.org/abs/1904.05160>.

Lu, S., Chai, J., and Wang, X. Neural collapse inspired debiased representation learning for min-max fairness. In *Proceedings of the 30th ACM SIGKDD Conference on Knowledge Discovery and Data Mining*, pp. 2048–2059, 2024.

Martin, A., Downing, J., Maden, M., Fleeman, N., Alfirevic, A., Haycox, A., and Pirmohamed, M. An assessment of the impact of pharmacogenomics on health disparities: a systematic literature review. *Pharmacogenomics*, 18(16):1541–1550, 2017.

Martinez, N., Bertran, M., and Sapiro, G. Minimax pareto fairness: A multi objective perspective. In III, H. D. and Singh, A. (eds.), *Proceedings of the 37th International Conference on Machine Learning*, volume 119 of *Proceedings of Machine Learning Research*, pp. 6755–6764. PMLR, 13–18 Jul 2020. URL <https://proceedings.mlr.press/v119/martinez20a.html>.

Martinez, N. L., Bertran, M. A., Papadaki, A., Rodrigues, M., and Sapiro, G. Blind pareto fairness and subgroup robustness. In Meila, M. and Zhang, T. (eds.), *Proceedings of the 38th International Conference on Machine Learning*, volume 139 of *Proceedings of Machine Learning Research*, pp. 7492–7501. PMLR, 18–24 Jul 2021. URL <https://proceedings.mlr.press/v139/martinez21a.html>.

Mas-Llado, C., Gonzalez-Del-Hoyo, M., Siquier-Padilla, J., Blaya-Peña, L., Coughlan, J., García de la Villa, B., Peral, V., and Rossello, X. Representativeness in randomised clinical trials supporting acute coronary syndrome guidelines. *European Heart Journal-Quality of Care and Clinical Outcomes*, 9(8):796–805, 2023.

McCoy, D., Zhang, W., Hubbard, A., van der Laan, M., and Schuler, A. Data-adaptive identification of effect modifiers through stochastic shift interventions and cross-validated targeted learning, 2024. URL <https://arxiv.org/abs/2406.10792>.

McCoy, R. T., Pavlick, E., and Linzen, T. Right for the wrong reasons: Diagnosing syntactic heuristics in natural language inference. *arXiv preprint arXiv:1902.01007*, 2019.

Musaogullari, A., Moorhead, J., Plana, A., and Johnson, A. Space for improvement: Zip codes should not determine cardiovascular longevity, a scoping review. *Trends in Cardiovascular Medicine*, 35(4):214–218, 2025. ISSN 1050-1738. doi: <https://doi.org/10.1016/j.tcm.2024.12.005>. URL <https://www.sciencedirect.com/science/article/pii/S1050173824001129>.

Nagarajan, V., Andreassen, A., and Neyshabur, B. Understanding the failure modes of out-of-distribution generalization, 2024. URL <https://arxiv.org/abs/2010.15775>.

Nam, J., Cha, H., Ahn, S., Lee, J., and Shin, J. Learning from failure: De-biasing classifier from biased classifier. *Advances in Neural Information Processing Systems*, 33: 20673–20684, 2020.

Oakden-Rayner, L., Dunnmon, J., Carneiro, G., and Ré, C. Hidden stratification causes clinically meaningful failures in machine learning for medical imaging, 2019. URL <https://arxiv.org/abs/1909.12475>.

Obermeyer, Z., Powers, B., Vogeli, C., and Mullainathan, S. Dissecting racial bias in an algorithm used to manage the health of populations. *Science*, 366(6464):447–453, 2019.

Qiu, S., Potapczynski, A., Izmailov, P., and Wilson, A. G. Simple and fast group robustness by automatic feature reweighting, 2023. URL <https://arxiv.org/abs/2306.11074>.

Raghavan, M., Barocas, S., Kleinberg, J., and Levy, K. Mitigating bias in algorithmic hiring: Evaluating claims and practices. In *Proceedings of the 2020 conference on fairness, accountability, and transparency*, pp. 469–481, 2020.

Ribeiro, M. T., Singh, S., and Guestrin, C. "why should i trust you?" explaining the predictions of any classifier. In *Proceedings of the 22nd ACM SIGKDD international conference on knowledge discovery and data mining*, pp. 1135–1144, 2016.

Rimsky, N., Gabrieli, N., Schulz, J., Tong, M., Hubinger, E., and Turner, A. Steering llama 2 via contrastive activation addition. In *Proceedings of the 62nd Annual Meeting of the Association for Computational Linguistics (Volume 1: Long Papers)*, pp. 15504–15522, 2024.

Rossello, X., Dominguez-Rodriguez, A., Latini, R., Sánchez, P. L., Raposeiras-Roubín, S., Anguita, M., Barrabés, J. A., Grigis, G., Owen, R., Pocock, S., et al. Beta-blockers after myocardial infarction: effects according to sex in the reboot trial. *European Heart Journal*, pp. ehaf673, 2025.

Rudner, T. G. J., Zhang, Y. S., Wilson, A. G., and Kempe, J. Mind the gap: Improving robustness to subpopulation shifts with group-aware priors, 2024. URL <https://arxiv.org/abs/2403.09869>.

Russakovsky, O., Deng, J., Su, H., Krause, J., Satheesh, S., Ma, S., Huang, Z., Karpathy, A., Khosla, A., Bernstein, M., et al. ImageNet Large Scale Visual Recognition Challenge. *International journal of computer vision*, 115(3):211–252, 2015.

Sagawa, S., Koh, P. W., Hashimoto, T. B., and Liang, P. Distributionally Robust Neural Networks For Group Shifts: On The Importance Of Regularization For Worst-Case Generalization. *International Conference on Learning Representations (ICLR)*, 2020.

Salaudeen, O., Zhang, H., Alhamoud, K., Beery, S., and Ghassemi, M. Aggregation hides out-of-distribution generalization failures from spurious correlations, 2025. URL <https://arxiv.org/abs/2510.24884>.

Santurkar, S., Tsipras, D., and Madry, A. Breeds: Benchmarks for subpopulation shift, 2020. URL <https://arxiv.org/abs/2008.04859>.

Sap, M., Card, D., Gabriel, S., Choi, Y., and Smith, N. A. The risk of racial bias in hate speech detection. In *Proceedings of the 57th annual meeting of the association for computational linguistics*, pp. 1668–1678, 2019.

Shah, H., Tamuly, K., Raghunathan, A., Jain, P., and Netrapalli, P. The pitfalls of simplicity bias in neural networks, 2020. URL <https://arxiv.org/abs/2006.07710>.

Shahamatdar, S., Saeed-Vafa, D., Linsley, D., Khalil, F., Lovinger, K., Li, L., McLeod, H. T., Ramachandran, S., and Serre, T. Deceptive learning in histopathology. *Histopathology*, 85(1):116–132, 2024.

Singla, S., Moayeri, M., and Feizi, S. Core risk minimization using salient imagenet. *arXiv preprint arXiv:2203.15566*, 2022.

Sohoni, N., Dunnmon, J., Angus, G., Gu, A., and Ré, C. No Subclass Left Behind: Fine-Grained Robustness In Coarse-Grained Classification Problems. *Neural Information Processing Systems (NeurIPS)*, 33:19339–19352, 2020.

To, M. N. N., RWilson, P. F., Nguyen, V., Harmanani, M., Cooper, M., Fooladgar, F., Abolmaesumi, P., Mousavi, P., and Krishnan, R. G. Diverse prototypical ensembles improve robustness to subpopulation shift, 2025. URL <https://arxiv.org/abs/2505.23027>.

Tsipras, D., Santurkar, S., Engstrom, L., Turner, A., and Madry, A. Robustness may be at odds with accuracy, 2019. URL <https://arxiv.org/abs/1805.12152>.

Tu, L., Lalwani, G., Gella, S., and He, H. An empirical study on robustness to spurious correlations using pre-trained language models. *CoRR*, abs/2007.06778, 2020. URL <https://arxiv.org/abs/2007.06778>.

Vogel, B., Acevedo, M., Appelman, Y., Merz, C. N. B., Chieffo, A., Figtree, G. A., Guerrero, M., Kunadian, V., Lam, C. S., Maas, A. H., et al. The lancet women and cardiovascular disease commission: reducing the global burden by 2030. *The Lancet*, 397(10292):2385–2438, 2021.

Wang, T., Sridhar, R., Yang, D., and Wang, X. Identifying and mitigating spurious correlations for improving robustness in nlp models, 2022. URL <https://arxiv.org/abs/2110.07736>.

Wang, Z., Qinami, K., Karakozis, I. C., Genova, K., Nair, P., Hata, K., and Russakovsky, O. Towards fairness in visual recognition: Effective strategies for bias mitigation. In *Proceedings of the IEEE/CVF conference on computer vision and pattern recognition*, pp. 8919–8928, 2020.

Williams, A., Nangia, N., and Bowman, S. R. A broad-coverage challenge corpus for sentence understanding through inference, 2018. URL <https://arxiv.org/abs/1704.05426>.

Wilson, K. and Caliskan, A. Gender, race, and intersectional bias in resume screening via language model retrieval. In *Proceedings of the AAAI/ACM Conference on AI, Ethics, and Society*, volume 7, pp. 1578–1590, 2024.

Winkler, J. K., Fink, C., Toberer, F., Enk, A., Deinlein, T., Hofmann-Wellenhof, R., Thomas, L., Lallas, A., Blum, A., Stolz, W., et al. Association between surgical skin markings in dermoscopic images and diagnostic performance of a deep learning convolutional neural network for melanoma recognition. *JAMA dermatology*, 155(10):1135–1141, 2019.

Wu, Z., Arora, A., Wang, Z., Geiger, A., Jurafsky, D., Manning, C. D., and Potts, C. Reft: Representation finetuning for language models. *Advances in Neural Information Processing Systems*, 37:63908–63962, 2024.

Yang, Y., Zhang, H., Katabi, D., and Ghassemi, M. Change is hard: A closer look at subpopulation shift, 2023. URL <https://arxiv.org/abs/2302.12254>.

Yang, Y., Zhang, H., Gichoya, J. W., Katabi, D., and Ghassemi, M. The limits of fair medical imaging ai in real-world generalization. *Nature Medicine*, 30(10):2838–2848, 2024a.

Yang, Y., Zhang, H., Katabi, D., and Ghassemi, M. On mitigating shortcut learning for fair chest x-ray classification under distribution shift. In *NeurIPS 2023 Workshop on Distribution Shifts: New Frontiers with Foundation Models*, 2024b.

Yao, H., Wang, Y., Li, S., Zhang, L., Liang, W., Zou, J., and Finn, C. Improving out-of-distribution robustness via selective augmentation, 2022. URL <https://arxiv.org/abs/2201.00299>.

Yin, F., Ye, X., and Durrett, G. Lofit: Localized fine-tuning on llm representations. *Advances in Neural Information Processing Systems*, 37:9474–9506, 2024.

Zech, J. R., Badgeley, M. A., Liu, M., Costa, A. B., Titano, J. J., and Oermann, E. K. Variable Generalization Performance Of A Deep Learning Model To Detect Pneumonia In Chest Radiographs: A Cross-Sectional Study. *PLoS medicine*, 15(11):e1002683, 2018.

Zhang, H., Cisse, M., Dauphin, Y. N., and Lopez-Paz, D. mixup: Beyond empirical risk minimization. *arXiv preprint arXiv:1710.09412*, 2017.

Zhang, H., Guo, Y., and Kankanhalli, M. Joint vision-language social bias removal for clip. In *Proceedings of the Computer Vision and Pattern Recognition Conference*, pp. 4246–4255, 2025.

Zhang, M., Sohoni, N. S., Zhang, H. R., Finn, C., and Ré, C. Correct-n-Contrast: A Contrastive Approach For Improving Robustness To Spurious Correlations. *Preprint arXiv 2203.01517v1*, 2022.

Zhao, D., Li, W., Shen, Z., Qiu, Y., Xu, B., Chen, H., and Chen, Y. Bias is a subspace, not a coordinate: A geometric rethinking of post-hoc debiasing in vision-language models. *arXiv preprint arXiv:2511.18123*, 2025.

Zhao, J., Wang, T., Yatskar, M., Ordonez, V., and Chang, K.-W. Men also like shopping: Reducing gender bias amplification using corpus-level constraints. *arXiv preprint arXiv:1707.09457*, 2017.

## Appendix Outline

This Appendix is organized as follows:

- In Appendix A, we provide code to illustrate the implementation of LEIA.
- In Appendix B, we provide motivation for the importance of unknown groups and evaluating under partial information of group relevance with the full proof for Proposition B.1 and details of the synthetic data experiment supporting the proposition.
- In Appendix C, we include details on datasets, baselines, and implementation with regards to hyperparameters and model training.
- In Appendix D, we demonstrate the robustness of LEIA to the gamma ( $\gamma$ ) hyperparameter and data splitting ratio, as well as a discussion of how  $\gamma$  is related to the underlying data distribution.
- In Appendix E, we provide a brief mathematical discussion on how and why LEIA works.
- In Appendix F, we discuss related work in more detail than the main text.

## A. Algorithm implementation details

In this section, we provide the code details of how we implement LEIA: how we compute error-informed weights based on prediction confidence; how the error-weighted covariance matrix is computed; how spectral decomposition identifies the error subspace ( $V_k$ ), and how the error subspace is applied to adjust classifier logits.

```

1 def compute_leia_weights(base_logits, y, gamma=10.0):
2     """
3         Compute LEIA weights that emphasize low-confidence
4             predictions.
5     """
6     probs = F.softmax(base_logits, dim=-1)
7
8     y_onehot = torch.zeros_like(base_logits).scatter_(
9         -1, y.unsqueeze(-1), 1
10    )
11    p_true = (probs * y_onehot).sum(-1)
12
13    log_weights = gamma * (1 - p_true)
14    log_weights = log_weights - log_weights.max()
15    weights = log_weights.exp()
16    weights = weights / weights.sum()
17
18    return weights.detach()

```

Listing 1. Computing LEIA error-informed weights

```

1 def explain_error_weighted_covariance(embeddings,
2     weights):
3     """
4         Compute the error-weighted covariance matrix
5     """
6     weights = weights / weights.sum()
7
8     mean_embedding = (weights.unsqueeze(-1) *
9         embeddings).sum(dim=0)
10    centered = embeddings - mean_embedding.unsqueeze(0)
11
12    covariance = (weights.unsqueeze(-1) * centered).T @
13        centered
14
15    return covariance, mean_embedding

```

Listing 2. Error-weighted covariance computation

```

1 def explain_spectral_decomposition(embeddings, weights,
2     k=1):
3     """
4         Identify the k-dimensional error subspace via
5             eigendecomposition.
6     """
7     covariance, _ = explain_error_weighted_covariance(
8         embeddings, weights
9     )
10
11    eigenvalues, eigenvectors =
12        torch.linalg.eigh(covariance)
13
14    idx = eigenvalues.argsort(descending=True)
15    eigenvalues = eigenvalues[idx]
16    eigenvectors = eigenvectors[:, idx]
17
18    V_k = eigenvectors[:, :k]
19    top_eigenvalues = eigenvalues[:k]
20
21    return V_k, top_eigenvalues

```

Listing 3. Spectral decomposition to identify the error subspace

```

1 class LEIAModel(nn.Module):
2     """
3         Low-rank Error-Informed Adjustment (LEIA) model.
4     """
5     def __init__(self, base_weight, base_bias, V_k):
6         super().__init__()
7         self.base_weight = base_weight
8         self.base_bias = base_bias
9         self.V_k = V_k
10
11        k, num_classes = V_k.shape[1],
12            base_weight.shape[0]
13        self.adjustment = nn.Parameter(
14            torch.zeros(k, num_classes)
15        )
16
17        def forward(self, embeddings):
18            base_logits = F.linear(
19                embeddings, self.base_weight, self.base_bias
20            )
21
22            projected = F.linear(
23                embeddings, self.V_k.t(), None
24            )
25
26            adjustment_logits = F.linear(
27                projected, self.adjustment.t(), None
28            )
29
30            return base_logits + adjustment_logits

```

Listing 4. LEIA model with low-rank error-informed adjustment

## B. Motivation for Unknown Groups Setting

### B.1. Proof of Proposition 3.3

For this section, we label hypotheses  $h, h'$  equal if and only if the subgroup risks for each group are all equal, i.e.  $h = h' \leftrightarrow \forall G : \mathcal{R}_G(h) = \mathcal{R}_G(h')$

**Lemma B.1.** *Let  $h_{\text{ERM}} \in \mathcal{H}$  be the Empirical Risk Minimizer among hypotheses classes. Then, for any  $h' \neq h_{\text{ERM}} \in \mathcal{H}$ , there must exist some group  $G$  such that  $\mathcal{R}_G(h') > \mathcal{R}_G(h_{\text{ERM}})$ .*

*Proof.* Suppose for contradiction that this was not the case, and for all  $G$  we had  $\mathcal{R}_G(h') \leq \mathcal{R}_G(h_{\text{ERM}})$ . Then, this would imply:

$$\begin{aligned} \forall G : \pi_G \mathcal{R}_G(h') &\leq \pi_G \mathcal{R}_G(h_{\text{ERM}}) \\ \sum_{G \in \mathcal{G}} \pi_G \mathcal{R}_G(h') &\leq \sum_{G \in \mathcal{G}} \pi_G \mathcal{R}_G(h_{\text{ERM}}) \end{aligned}$$

Moreover, by our assumption that  $h' \neq h_{\text{ERM}}$ , one of the individual group inequalities must be strict, meaning the second inequality is also strict. But this violates the optimality of  $h_{\text{ERM}}$ , as by definition it is  $\arg \min_{h \in \mathcal{H}} \sum_{G \in \mathcal{G}} \pi_G \mathcal{R}_G(h)$ . Thus, a group with our desired properties must exist.  $\square$

### Main proposition:

*Proof.* Let  $h_{\text{DRO+}} \in \mathcal{H}_{\text{DRO}}(\mathcal{G})$  be an output of running Group DRO with all subgroups known. Assume for now that  $h_{\text{DRO+}} \neq h_{\text{ERM}}$ . From B.1, we can find a group  $G$  such that  $\mathcal{R}_G(h_{\text{DRO+}}) > \mathcal{R}_G(h_{\text{ERM}})$ . We now claim that the proposition holds with  $i$  being the index of this group.

Assume that (i) does not hold, and we shall show that (ii) must be true. Sample  $h_{\text{DRO}} \in \mathcal{H}_{\text{DRO}}(\mathcal{G} \setminus \{G_i\})$ . We do casework based on the worst subgroup risk among explicitly optimized-for groups for  $h_{\text{DRO}}$  and  $h_{\text{DRO+}}$ .

**Case 1:**  $\max_{G \in \mathcal{G} \setminus \{G_i\}} \mathcal{R}_G(h_{\text{DRO}}) < \max_{G \in \mathcal{G}} \mathcal{R}_G(h_{\text{DRO+}})$

Suppose further in this case that  $\mathcal{R}_{G_i}(h_{\text{DRO}}) < \mathcal{R}_{G_i}(h_{\text{DRO+}})$ . We would then have:

$$\begin{aligned} &\max_{G \in \mathcal{G}} \mathcal{R}_G(h_{\text{DRO}}) \\ &= \max\{\mathcal{R}_{G_i}(h_{\text{DRO}}), \max_{G \in \mathcal{G} \setminus \{G_i\}} \mathcal{R}_G(h_{\text{DRO}})\} \\ &< \max\{\mathcal{R}_{G_i}(h_{\text{DRO+}}), \max_{G \in \mathcal{G}} \mathcal{R}_G(h_{\text{DRO+}})\} \\ &= \max_{G \in \mathcal{G}} \mathcal{R}_G(h_{\text{DRO+}}) \end{aligned}$$

where the inequality comes from the fact that strict inequality is assumed for each pair of arguments. However, this violates the definitional optimality of  $h_{\text{DRO+}}$ , and consequently, we must have  $\mathcal{R}_{G_i}(h_{\text{DRO}}) \geq \mathcal{R}_{G_i}(h_{\text{DRO+}})$ . Putting it all together, we have  $\mathcal{R}_{G_i}(h_{\text{DRO}}) \geq \mathcal{R}_{G_i}(h_{\text{DRO+}}) > \mathcal{R}_{G_i}(h_{\text{ERM}})$

**Case 2:**  $\max_{G \in \mathcal{G} \setminus \{G_i\}} \mathcal{R}_G(h_{\text{DRO}}) = \max_{G \in \mathcal{G}} \mathcal{R}_G(h_{\text{DRO+}})$

Here, we have  $h_{\text{DRO+}} \in \mathcal{H}_{\text{DRO}}(\mathcal{G} \setminus \{G_i\})$ ; i.e. it also minimizes the Group DRO objective with  $G_i$  treated as an unknown group. By our assumptions, this directly satisfies (ii).

Finally, we take care of the case where  $h_{\text{DRO+}} = h_{\text{ERM}}$ . Splitting up the work into the same two cases - in the first, we can directly apply B.1 to  $h_{\text{DRO}}$ ; and for the second, note that the first condition would hold in this case. This completes the proof.  $\square$

## B.2. Synthetic Data Experiment

We generate synthetic data with  $N$  known subgroups and one unknown subgroup (indexed as group 0), where each group exhibits conflicting spurious correlations. Each example has seven features in total: five stable features sampled from a standard Gaussian distribution  $\mathcal{N}(0, I)$  that determine the true label, and two spurious features that induce group-specific correlations. Binary labels are generated as

$$y = \text{sign}(\theta^\top x_{\text{stable}} + \epsilon),$$

where  $\theta$  is a randomly sampled unit vector scaled to signal strength 1.5,  $x_{\text{stable}} \in \mathbb{R}^5$  denotes the stable features, and  $\epsilon \sim \mathcal{N}(0, 0.8^2)$  is Gaussian label noise. The unknown subgroup (group 0), with size ratio  $\rho$  relative to each known group, has spurious feature 0 strongly correlated with the label (strength 4.5) and spurious feature 1 anti-correlated (strength 3.0). In contrast, the known subgroups (groups 1 through  $N$ , with 1000 samples each) exhibit the opposite pattern: spurious feature 1 is positively correlated with the label (strength 4.0), while spurious feature 0 is anti-correlated (strength 3.0). Spurious features are generated deterministically from the labels with added Gaussian noise ( $\sigma = 0.5$ ), creating a setting in which optimizing performance on known groups induces systematic errors on the unknown group. We split the dataset into 60% training, 20% validation, and 20% test sets. We train three linear classifiers, each consisting of a single fully connected layer mapping from seven input features to two output classes: (1) ERM, which minimizes the average cross-entropy loss across all training data using SGD (learning rate 0.01, momentum 0.9, batch size 64) for 100 epochs, (2) Group DRO, which is trained on all data but updates adversarial group weights only for the known groups, assigning zero loss weight to the unknown group, with step size  $\eta = 0.01$ , and (3) LEIA with rank  $k = 1$ ,  $\gamma = 100$ , and no regularization coefficient. Both models observe the same training data; however, Group DRO updates its group weights exclusively based on losses from known groups. For LEIA, we do not use early stopping or hyperparameter tune. We evaluate the three methods on all groups, including the unknown subgroup, to demonstrate that robustness optimization over known groups can lead to degraded performance on previously unseen subgroups relative to ERM. Results are averaged over three seeds (0, 1, and 42).

Table 5. Unknown-group accuracy (UGA) across synthetic parameter sweeps.  $N$  denotes the number of known groups and  $\rho$  denotes the unknown group size ratio. UGA is reported for ERM and Group DRO. Harm is defined as the percentage-point decrease in UGA when using Group DRO relative to ERM.

$N$	$\rho$	ERM UGA (%)	GDRO UGA (%)	Harm (%)	LEIA UGA (%)
1	0.1	77.5 $\pm$ 15.5	55.4 $\pm$ 7.2	22.1 $\pm$ 8.5	85.5 $\pm$ 11.0
	0.2	84.9 $\pm$ 0.4	49.1 $\pm$ 9.0	35.8 $\pm$ 9.2	91.5 $\pm$ 7.8
	0.3	85.1 $\pm$ 4.7	44.8 $\pm$ 4.8	40.3 $\pm$ 9.1	86.9 $\pm$ 7.6
2	0.1	58.3 $\pm$ 7.6	42.5 $\pm$ 5.9	15.9 $\pm$ 3.6	71.0 $\pm$ 19.0
	0.2	82.3 $\pm$ 4.0	42.2 $\pm$ 11.2	40.1 $\pm$ 8.8	89.6 $\pm$ 4.8
	0.3	75.6 $\pm$ 4.9	49.8 $\pm$ 9.1	25.8 $\pm$ 13.3	88.7 $\pm$ 1.4
3	0.1	63.6 $\pm$ 8.8	49.4 $\pm$ 9.2	14.2 $\pm$ 2.2	55.3 $\pm$ 11.5
	0.2	74.8 $\pm$ 13.5	57.2 $\pm$ 8.9	17.6 $\pm$ 7.6	76.2 $\pm$ 10.0
	0.3	65.6 $\pm$ 3.9	43.4 $\pm$ 1.0	22.3 $\pm$ 2.9	74.8 $\pm$ 18.5
4	0.1	66.2 $\pm$ 4.4	60.2 $\pm$ 7.4	6.0 $\pm$ 6.3	64.1 $\pm$ 4.1
	0.2	61.5 $\pm$ 3.6	51.3 $\pm$ 8.2	10.2 $\pm$ 4.8	79.9 $\pm$ 19.7
	0.3	73.0 $\pm$ 10.9	50.8 $\pm$ 4.8	22.2 $\pm$ 6.3	90.2 $\pm$ 6.6

## C. Experimental settings

### C.1. Datasets

Our works makes use of five datasets across various types of group robustness challenges.

**WATERBIRDS** (Sagawa et al., 2020) is an image classification benchmark whose task is to classify birds as ‘waterbirds’ (birds that frequent water) or ‘landbirds’ (birds that do not). The dataset is an example of *spurious correlations*: waterbirds often appears in images with water, while landbirds do not, causing models to often fail to classify waterbirds without water backgrounds or landbirds with water backgrounds.

**CELEBA** (Liu et al., 2015) is an image classification benchmark whose task is to classify celebrities as blond or not blond. The dataset is an example of *attribute imbalance*, as blond hair is found more frequently in females, making it hard to correctly identify blond males or non-blond females.

**MULTINLI** (Williams et al., 2018) is a text classification dataset where models must predict the relationship between

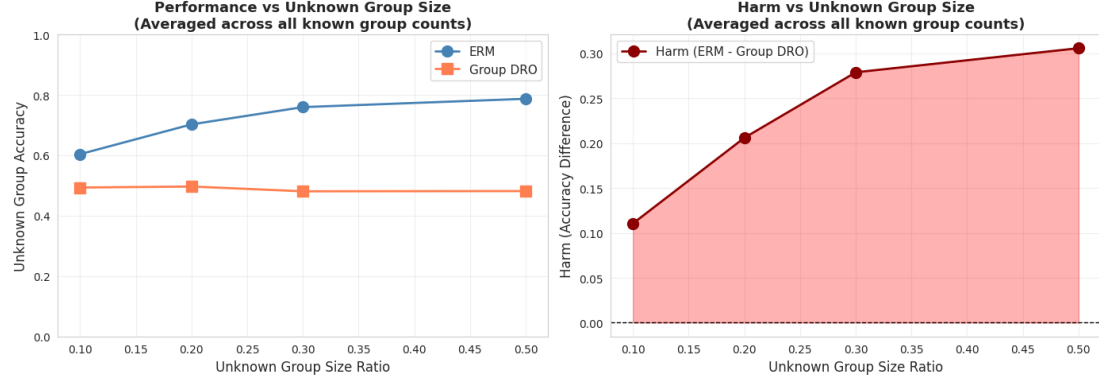


Figure 5. Performance trends as a function of unknown group size ratio. Left: Unknown group accuracy for ERM and Group DRO averaged across all numbers of known groups. ERM accuracy improves with larger unknown group size (more training data), while Group DRO accuracy remains relatively constant or decreases. Right: Harm (ERM - Group DRO) increases monotonically with unknown group size ratio, demonstrating that Group DRO's strategy of ignoring unknown groups becomes increasingly problematic as unknown groups become more prevalent in the data.

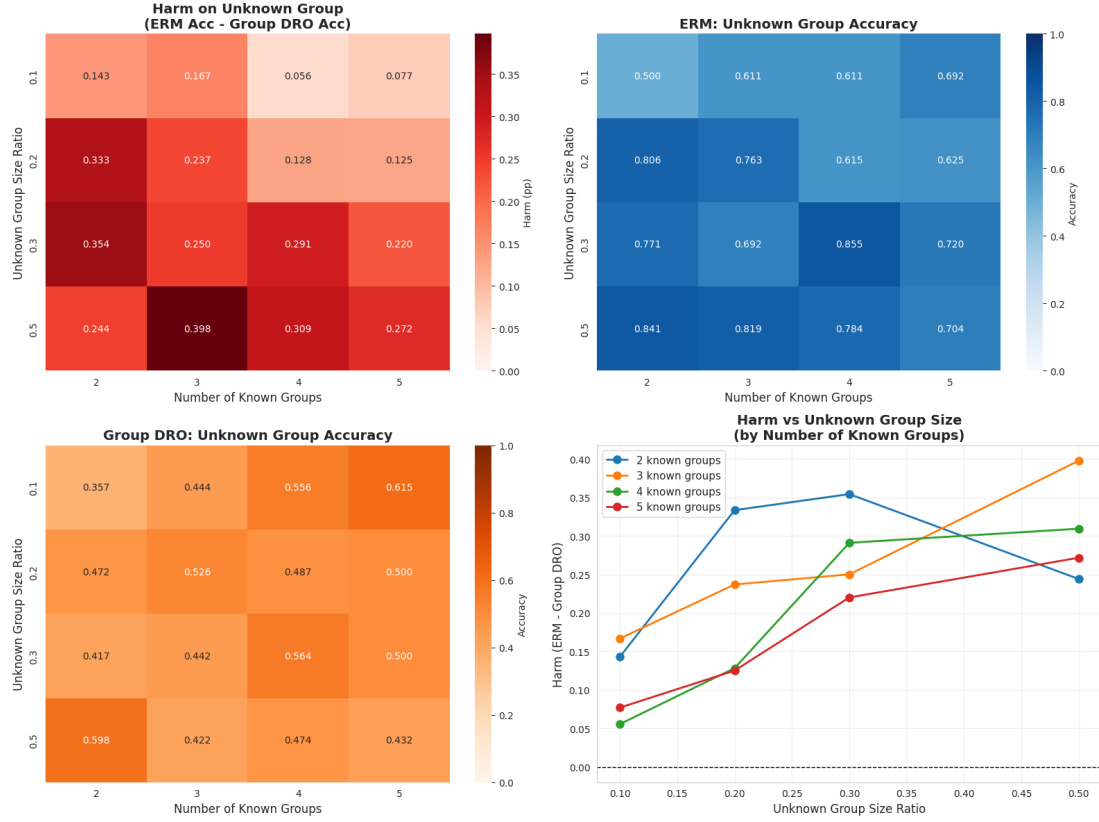


Figure 6. Performance on unknown subgroups across parameter settings. Heatmaps showing (top-left) harm on unknown groups (ERM accuracy minus Group DRO accuracy), (top-right) ERM accuracy on unknown groups, (bottom-left) Group DRO accuracy on unknown groups, and (bottom-right) harm as a function of unknown group size ratio for different numbers of known groups. Results are from synthetic experiments with 2-5 known groups and unknown group size ratios of 0.1-0.5. Warmer colors indicate higher values. The harm increases with unknown group size ratio, demonstrating that Group DRO's strategy of ignoring unknown groups becomes more problematic as unknown groups become more prevalent in the data.

two sentences from the possibilities of ‘entailment’, ‘contradiction’, or ‘neutral’. This dataset is an example of *spurious correlations*: many examples of the ‘contradiction’ label contain negations, which may cause models to associate the presence of these erroneously with contradictions.

Table 6. Example inputs from datasets

Dataset	Examples					
<i>Image datasets</i>						
Waterbirds						
CelebA						
CheXpert						
<i>Text datasets</i>						
CivilComments	<p>“Munchins looks like a munchins. The man who dont want to show his taxes, will tell you everything...”</p> <p>“The democratic party removed the filibuster to steamroll its agenda. Suck it up boys and girls.”</p> <p>“so you dont use oil? no gasoline? no plastic? man you ignorant losers are pathetic.”</p>					
MultiNLI	<p>“The analysis proves that there is no link between PM and bronchitis.”</p> <p>“Postal Service were to reduce delivery frequency.”</p> <p>“The famous tenements (or lands) began to be built.”</p>					

**CIVILCOMMENTS** (Borkan et al., 2019) is a text classification dataset whose task is to classify online comments as ‘toxic’ and ‘non-toxic’. We use the version from the WILDS benchmark (Koh et al., 2021). The comments are tagged with mentioned demographic group. This dataset is an example of *class imbalance*: some of these groups are underrepresented, and models run the risk of associating group membership with the solution to the classification task.

**CHEXPERT** (Irvin et al., 2019) is a dataset of chest radiographs where the task is to predict whether or not there are abnormalities. The dataset is an example of significant *class imbalance*, as some conditions (varieties of abnormalities) are not frequently found in the training dataset.

## C.2. Baselines

**Empirical Risk Minimization (ERM)** optimizes for average performance across the entire training distribution. While effective in balanced settings, ERM is prone to prioritizing majority-group characteristics, often at the expense of performance on underrepresented subpopulations. By optimizing a global average, ERM is frequently susceptible to spurious correlations and performance degradation under subpopulation shift.

**Classifier Re-train (CRT, ReWeightCRT)** (Kang et al., 2020) decouples representation learning from classifier learning by first training a feature extractor using standard ERM, then retraining the classifier with class-balanced reweighting or resampling. This improves performance on underrepresented classes without modifying the learned representation.

**Just Train Twice (JTT)** (Liu et al., 2021) is a two-stage method that first trains a model using ERM to identify hard examples, defined as samples misclassified by the initial model. In the second stage, the model is retrained while upweighting these hard examples, improving robustness to spurious correlations and subpopulation shifts.

**Mixup** (Zhang et al., 2017) is a simple, data-agnostic augmentation technique that constructs virtual training examples via convex combinations of pairs of inputs and labels. By encouraging the model to behave linearly between examples, Mixup implicitly regularizes the decision boundary, improves generalization, and reduces sensitivity to spurious correlations.

**LISA** (Yao et al., 2022) improves out-of-distribution robustness by applying Mixup selectively across specific groups. LISA alternates between intra-label LISA, which interpolates samples with the same label but different domains to cancel out domain-specific noise, and intra-domain LISA, which interpolates samples within the same domain but with different

labels to force the model to ignore domain-wide biases. This encourages the learning of invariant predictors that generalize better to subpopulation and domain shifts.

**Deep Feature Reweighting (DFR)** (Kirichenko et al., 2022) first trains a model via standard ERM on the full dataset to develop a robust feature extractor using only the dataset and labels. Then, the classification head is discarded and a new one is trained from scratch using a balanced validation set, requiring group information.

**Diverse Prototypical Ensembles (DPE)** (To et al., 2025) addresses subpopulation shifts by replacing the standard linear classification head with an ensemble of diversified, distance-based prototype classifiers.

DPE employs an explicit inter-prototype similarity loss to enforce functional diversity among ensemble members. This allows the model to capture multiple distinct decision boundaries, effectively discovering and representing latent subpopulations even when group annotations or distributions are unknown.

**Correct-n-Contrast (CnC)** (Zhang et al., 2022) is a two-stage framework designed to improve worst-group performance by leveraging contrastive learning without explicit group labels. In the first stage, a standard ERM model is trained to identify samples prone to spurious correlations, using its predictions as proxies for latent group attributes. In the second stage, the model is trained using a supervised contrastive loss that treats samples with the same class but different proxy attributes as “positives” (to be pulled together) and samples with different classes but the same proxy attributes as “negatives” (to be pushed apart). This forces the encoder to prioritize class-invariant features while ignoring the spurious attributes identified in the first stage.

**Automatic Feature Reweighting (AFR)** (Qiu et al., 2023) is a last-layer retraining method designed to reduce a model’s reliance on spurious correlations. AFR updates the classification head of a pre-trained ERM model using a weighted loss that automatically emphasizes examples where the initial model performs poorly. By upweighting these “hard” examples, which typically correspond to minority subpopulations, AFR improves robustness to distribution shifts without requiring explicit group annotations or expensive retraining of the entire network.

**Group Inference via data Comparison (GIC)** (Han & Zou, 2024) is a group inference framework that identifies latent spurious attributes by leveraging two datasets with differing group distributions. It trains a spurious attribute classifier based on two key properties of spurious correlations: (1) spurious attributes are highly predictive of the label, and (2) the strength of this predictiveness varies across datasets with different group proportions. By encouraging inferred attributes that exhibit dataset-dependent label correlations, GIC produces more accurate pseudo group labels, which can then be used by downstream robust learning algorithms to improve worst-group performance.

**Invariant Risk Minimization (IRM)** (Arjovsky et al., 2019) aims to learn predictors whose performance is stable across multiple training environments, thereby promoting out-of-distribution generalization. IRM formalizes this by seeking a data representation such that the optimal classifier on top of that representation is simultaneously optimal for all environments, effectively isolating invariant correlations while ignoring spurious ones.

**Conditional Value-at-Risk DRO (CVaRDRO)** (Duchi & Namkoong, 2020) proposes a distributionally robust optimization variant that dynamically upweights samples with the highest losses without requiring explicit group annotations. Based on the Conditional Value-at-Risk (CVaR) objective, this method focuses optimization on the tail of the loss distribution, which often correspond to minority subpopulations or examples misaligned with spurious correlations.

**Group DRO** (Sagawa et al., 2020) improves subpopulation robustness by minimizing a surrogate objective that upper-bounds the worst-group loss. Instead of optimizing average empirical risk, it maintains group-level weights (requiring explicit group annotations) and dynamically upweights groups with higher loss during training.

### C.3. Implementation

In this section, we provide specific implementation details to reproduce our results. First, we include LEIA-specific information with the two stage training. For the stage 1 ERM training (see Table 7), we follow ERM generated used in the Automatic Feature Reweighting (AFR) (Qiu et al., 2023) for the WATERBIRDS, CELEBA, CIVILCOMMENTS, and MULTINLI datasets. For CHEXPERT, we use the SubpopBench (Yang et al., 2023) implementation of ERM till convergence.

Table 7. LEIA Stage 1 ERM Training Configuration for All Datasets

Dataset	Architecture	Epochs	Batch Size	Learning Rate	Weight Decay	Scheduler	Optimizer
WATERBIRDS	ResNet-50 (ImageNet)	50	32	0.003	$1 \times 10^{-4}$	Constant	SGD
CELEBA	ResNet-50 (ImageNet)	20	100	0.003	$1 \times 10^{-4}$	Cosine	SGD
CIVILCOMMENTS	BERT-base-uncased	3	32	$2 \times 10^{-5}$	0.0	Constant	AdamW
MULTINLI	BERT-base-uncased	3	32	$2 \times 10^{-5}$	0.0	Constant	AdamW
CHEXPERT	ResNet-50 (ImageNet)	13*	108	0.001	$1 \times 10^{-4}$	Default**	SGD

\* CheXpert uses 20,001 training steps (approximately 13 epochs with batch size 108).

\*\* CheXpert uses SubpopBench’s default scheduler configuration.

Table 8. LEIA Stage 2 Hyperparameter Configurations Across Datasets

Dataset	Epochs	Gamma Values	Rank Values
WATERBIRDS	100	7.5, 8.5	4, 16, 32
CELEBA	100	0.5, 0.75, 1.25, 1.5	2, 4, 12, 36, 52
CIVILCOMMENTS	50	500, 1000, 5000	1, 4, 5
MULTINLI	50	200, 500, 1000	1, 2, 3
CHEXPERT	50	0.5, 1, 1.5	50, 52, 54

**Note:** Across all datasets, the regularization coefficient (`reg_coeff`) is set to 0.0 and the learning rate is 0.02.

For the no group information setting and complete group information, asterisked results in Tables 1 and 11 reproduce results from SubpopBench’s implementation (Yang et al., 2023). DPE, GIC, AFR, and CnC results are from the methods’ papers respectively (To et al., 2025; Han & Zou, 2024; Qiu et al., 2023; Zhang et al., 2022). In the setting with complete information of group relevance, the JTT, LISA, DFR, and GroupDRO results are from the methods’ papers respectively (Liu et al., 2021; Yao et al., 2022; Kirichenko et al., 2022; Sagawa et al., 2020).

For the partial group setting, we provide complete details on all the hyperparameter tuning for baselines. To ensure fair comparison between LEIA and baseline, we ensure sufficient tuning by considering configurations from SubpopBench and original papers. Note that we do early stopping on the validation worst group accuracy with known groups, making epochs not as important to tune across methods and having long training horizons to ensure we train till convergence.

#### C.4. Runtime Analysis

We provide Table 10 to accompany Figure 3 to clearly show the differences between baselines. Timings are obtained by are obtained by running on a single RTX8000 (48 GB) NVIDIA GPU. As with prior work (Qiu et al., 2023), we included the time to pre-compute and cache the embeddings, which in practice can be ignored by amortizing across a hyperparameter sweep.

## D. Additional results

### D.1. Additional Baselines for Complete Information of Group Relevancy Setting

We provide the results of DFR, DPE, Group DRO, IRM, and LISA in this table for maximum completeness.

### D.2. Ablation to $\gamma$ parameter

Beyond rank robustness, LEIA is also robust to the choice of the reweighting strength hyperparameter  $\gamma$ . Different datasets exhibit different optimal  $\gamma$  values image datasets typically favor  $\gamma \approx 1\text{--}8$ , whereas text datasets require larger values around  $\gamma \approx 500\text{--}5000$ . Figure 7 shows that performance remains stable across a broad neighborhood of these optima. For each  $\gamma$ , we select the best rank based on validation worst-group accuracy (WGA) and report the mean  $\pm$  one standard deviation across seeds.

Across all datasets, LEIA performance varies by less than 2–3 percentage points over the tested  $\gamma$  ranges, despite optimal values differing by orders of magnitude. This robustness arises from the exponential weighting scheme,  $\mu_i = \exp(\gamma(1-p_i))$ , which induces meaningful relative weight differences over a wide range of  $\gamma$  values. Together with our analysis linking

Table 9. Hyperparameter Sweep Configurations for Baseline Methods (CIVILCOMMENTS &amp; CHEXPERT)

Method	Search Type	Trials	Epochs	Learning Rate	Hyperparameters
LEIA	Grid	10	100	$2 \times 10^{-2}$	$\gamma \in [100, 1000], k \in [1, 4, 5, 6, 9], \lambda = 0$
AFR (CC)	Grid	12	100	$3 \times 10^{-3}$	$\gamma \in [0, 0.01, 0.1, 1, 3, 10], \lambda \in [0.0, 1 \times 10^{-2}]$
AFR (CX)	Grid	32	100	$[10^{-4}, 10^{-3}, 10^{-2}, 5 \times 10^{-2}]$	$\gamma \in [1, 2, 4, 6], \lambda \in [0.0, 1 \times 10^{-2}]$
DFR (CC)	Random	25	100	$1 \times 10^{-2}$	$\text{dfr.reg} \sim 10^{\text{Uniform}(-2.0, 0.5)}$
DFR (CX)	Random	25	100	$1 \times 10^{-2}$	$\text{dfr.reg} \sim 10^{\text{Uniform}(-0.5, 0.5)}$
CRT	None	1	100	$1 \times 10^{-2}$	None
Reweighting	None	1	100	$1 \times 10^{-2}$	None
JTT	Random	25	100	$1 \times 10^{-5}$	$\text{step\_frac} \sim \text{Uniform}(0.2, 0.8), \lambda \sim 10^{\text{Uniform}(0, 2.5)}, \text{wd} = 0.1 \text{ (Stage 1 \& 2)}$
LISA	Random	25	100	$1 \times 10^{-2}$	$\alpha \sim 10^{\text{Uniform}(-1, 1)}, p_{\text{sel}} \sim \text{Uniform}(0, 1)$
IRM	Random	25	100	$1 \times 10^{-2}$	$\lambda \sim 10^{\text{Uniform}(-1.5)}, \text{iters} \sim 10^{\text{Uniform}(0, 4)}$
CVaRDRO	Random	25	100	$1 \times 10^{-2}$	$\alpha \sim 10^{\text{Uniform}(-2, 0)}$
Mixup	Random	25	100	$1 \times 10^{-2}$	$\alpha \sim 10^{\text{Uniform}(0, 4)}$
GroupDRO	None	1	100	$1 \times 10^{-2}$	$\eta = 1 \times 10^{-2}$
ERM	None	1	100	$1 \times 10^{-2}$	None

**Notes:**

- LEIA:  $\gamma$  = reweighting strength,  $k$  = spectral rank
- AFR:  $\gamma$  = reweighting strength,  $\lambda$  = regularization coefficient
- DFR: dfr.reg = L1 regularization on classifier weights
- JTT: step\_frac = fraction of epochs for Stage 1,  $\lambda$  = upweighting factor for misclassified examples
- LISA:  $\alpha$  = mixup Beta parameter,  $p_{\text{sel}}$  = selection probability
- IRM:  $\lambda$  = penalty weight, iters = penalty annealing iterations
- CVaRDRO:  $\alpha$  = uncertainty set size (CVaR parameter)
- Mixup:  $\alpha$  = mixup Beta parameter
- GroupDRO:  $\eta$  = group weight update rate

Table 10. End-to-end Runtime Comparison (minutes)

Dataset	ERM	LEIA	AFR	JTT	DPE	GIC
WATERBIRDS	25.05	26.53	26.58	76.08	40.12	120.20
CELEBA	158.36	167.03	169.27	479.71	254.00	767.24
CIVILCOMMENTS	145.95	164.89	166.68	441.85	257.51	757.72
MULTINLI	61.23	72.99	73.12	185.52	116.33	335.29

optimal  $\gamma$  to dataset-specific confidence distributions, these results demonstrate that LEIA is practical to deploy: practitioners can initialize  $\gamma$  using coarse, dataset-appropriate values and fine-tune within a forgiving range.

Taken together, the rank and  $\gamma$  robustness analyses show that LEIA has two relatively forgiving hyperparameters, making it substantially easier to use than methods that require precise hyperparameter tuning.

Like  $k$ , we also observe that optimal  $\gamma$  values vary based on the underlying dataset distribution. The hyperparameter  $\gamma$  in LEIA controls the strength of exponential reweighting based on model uncertainty. Specifically, LEIA assigns each training example a weight  $\mu_i = \exp(\gamma(1 - p_i))$ , where  $(1 - p_i)$  represents the model's uncertainty for example  $i$ . The parameter  $\gamma$  acts as a scaling factor: larger values amplify small differences in uncertainty into larger weight disparities, while smaller values yield more uniform weighting. As a result, the optimal choice of  $\gamma$  is fundamentally tied to the distribution of uncertainties in the dataset, as it must induce meaningful weight differentiation over the typical range of uncertainty values.

Uncertainty distributions vary substantially across dataset (see Figure 8). Most examples in image datasets such as CELEBA and WATERBIRDS have near-zero uncertainty, reflecting high model confidence, alongside a distinct tail of higher-uncertainty examples (95th percentile  $\approx 0.4$ – $0.8$ ). Relatively small values of  $\gamma$  (1–8) are sufficient, as the separation between the bulk and the tail allows even modest scaling to produce meaningful weight differences between confident examples. In contrast, text datasets such as CIVILCOMMENTS and MULTINLI display continuous, compressed distributions: uncertainties are small but non-zero for most examples (median  $\approx 0.002$ – $0.019$ ), with values concentrated in a narrow range (interquartile

**Table 11. Worst-group accuracy (WGA) and average accuracy on the test set with complete information of group relevance.** Baselines are divided into two types based on whether group labels are used for training the method. Rows denoted with asterisks (\*) and CheXpert results reproduces baselines (Yang et al., 2023). Other results are reported from original papers of competitive baselines. Group Info (Train/Val) indicates whether group labels are used:  $\times$  = no group info used,  $\star$  = group info used for hyperparameter tuning and early stopping,  $\checkmark$  = group info used for training. Best and second-best values within each half are **bold** and underlined, respectively. “-” indicates results not reported. All of our results are the mean  $\pm$  standard deviation (in %) averaged over three independent runs.

Algorithm	Group Info (Train/Val)	WATERBIRDS		CELEBA		CIVILCOMMENTS		MULTINLI		CHEXPERT	
		WGA	Avg Acc	WGA	Avg Acc	WGA	Avg Acc	WGA	Avg Acc	WGA	Avg Acc
<i>Group labels are not used for training</i>											
ERM*	$\times/\star$	69.1 $\pm$ 4.7	84.1 $\pm$ 1.7	57.6 $\pm$ 0.8	<u>95.0</u> $\pm$ 0.1	63.2 $\pm$ 1.2	85.4 $\pm$ 0.2	69.5 $\pm$ 0.3	80.9 $\pm$ 0.3	41.7 $\pm$ 3.4	<b>88.6</b> $\pm$ 0.7
CRT*	$\times/\star$	76.3 $\pm$ 0.8	89.2 $\pm$ 0.1	70.4 $\pm$ 0.4	94.1 $\pm$ 0.1	68.5 $\pm$ 0.0	83.0 $\pm$ 0.0	65.4 $\pm$ 0.1	80.2 $\pm$ 0.0	74.0 $\pm$ 0.2	79.1 $\pm$ 0.1
ReWeightCRT*	$\times/\star$	76.3 $\pm$ 0.2	89.4 $\pm$ 0.3	71.1 $\pm$ 0.5	94.2 $\pm$ 0.1	68.2 $\pm$ 0.4	83.4 $\pm$ 0.0	65.3 $\pm$ 0.1	80.2 $\pm$ 0.0	73.9 $\pm$ 0.2	79.0 $\pm$ 0.1
JTT	$\times/\star$	86.7	93.3	81.1	88.0	69.3	<b>91.1</b>	72.6	78.6	60.4 $\pm$ 4.8	75.2 $\pm$ 0.8
CVaRDRO*	$\times/\star$	75.5 $\pm$ 2.2	89.9 $\pm$ 0.4	62.2 $\pm$ 3.1	95.1 $\pm$ 0.1	68.7 $\pm$ 1.3	83.5 $\pm$ 0.3	63.0 $\pm$ 1.5	75.1 $\pm$ 0.1	50.2 $\pm$ 1.8	73.7 $\pm$ 1.0
CnC	$\times/\star$	88.5 $\pm$ 0.3	90.9 $\pm$ 0.1	<u>88.8</u> $\pm$ 0.9	89.9 $\pm$ 0.5	68.9 $\pm$ 2.1	81.7 $\pm$ 0.5	—	—	—	—
AFR	$\times/\star$	<u>90.4</u> $\pm$ 1.1	<b>94.2</b> $\pm$ 1.2	82.0 $\pm$ 0.5	91.3 $\pm$ 0.3	68.7 $\pm$ 0.6	89.8 $\pm$ 0.6	<b>73.4</b> $\pm$ 0.6	<u>81.4</u> $\pm$ 0.2	—	—
GIC	$\times/\star$	86.3 $\pm$ 0.1	89.6 $\pm$ 1.3	<b>89.4</b> $\pm$ 0.2	91.9 $\pm$ 0.1	<u>72.5</u> $\pm$ 0.3	90.0 $\pm$ 0.3	—	—	—	—
LEIA (Ours)	$\times/\star$	<b>90.7</b> $\pm$ 0.2	<u>93.3</u> $\pm$ 0.7	85.0 $\pm$ 0.9	<b>95.2</b> $\pm$ 0.1	<b>72.9</b> $\pm$ 0.2	90.9 $\pm$ 0.8	69.6 $\pm$ 0.8	<b>81.4</b> $\pm$ 0.4	<b>75.2</b> $\pm$ 0.3	79.6 $\pm$ 0.3
<i>Group labels are used for training</i>											
DFR	$\times/\checkmark/\checkmark$	92.9 $\pm$ 0.4	94.2 $\pm$ 0.4	88.3 $\pm$ 1.1	91.3 $\pm$ 0.3	70.1 $\pm$ 0.8	87.2 $\pm$ 0.3	74.7 $\pm$ 0.7	82.1 $\pm$ 0.2	71.7 $\pm$ 0.2	78.2 $\pm$ 0.4
DPE	$\times/\checkmark$	91.0 $\pm$ 0.4	92.5 $\pm$ 0.2	89.8 $\pm$ 0.2	<u>87.7</u> $\pm$ 0.6	82.2 $\pm$ 0.2	71.5 $\pm$ 0.6	81.3 $\pm$ 0.2	74.8 $\pm$ 0.3	—	—
Group DRO	$\checkmark/\star$	91.4	93.5	88.9	92.9	77.7	81.4	69.9	88.9	74.5 $\pm$ 0.2	78.9 $\pm$ 0.3
IRM*	$\checkmark/\star$	74.5 $\pm$ 1.5	88.4 $\pm$ 0.1	63.0 $\pm$ 2.5	94.7 $\pm$ 0.8	63.2 $\pm$ 0.8	85.5 $\pm$ 0.0	63.6 $\pm$ 1.3	77.8 $\pm$ 0.6	34.4 $\pm$ 1.7	89.8 $\pm$ 0.3
LISA	$\checkmark/\star$	89.2	91.8	89.3	92.4	72.6	89.2	—	—	75.6 $\pm$ 0.6	79.2 $\pm$ 0.8

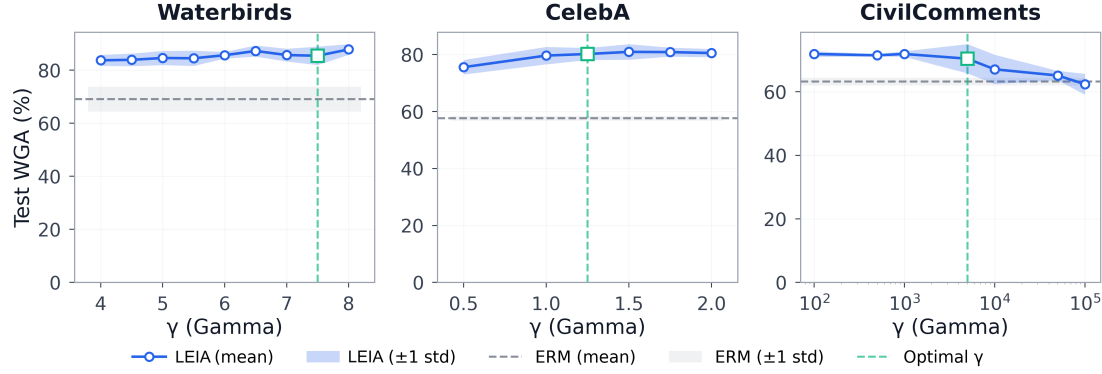


**Figure 7. LEIA Robustness to Gamma ( $\gamma$ ) Selection.** Test worst-group accuracy (WGA) as a function of gamma for WATERBIRDS, CELEBA, AND CIVILCOMMENTS. For each gamma value, we select the best rank (by validation WGA) and report mean  $\pm$  1 standard deviation across seeds. The green dashed line and diamond marker indicate the empirically-observed optimal gamma for each dataset. The gray dashed line and shaded region show ERM performance (mean  $\pm$  1 std). LEIA demonstrates robustness to gamma selection, with performance remaining stable across a reasonable range around the optimal values.

range spanning approximately 0.0005–0.03). Much larger values of  $\gamma$  (500–5000) are required to amplify small differences in uncertainty.

### D.3. Robustness to data splitting ratio

We assess how robust our method is to the data splitting ratio used for  $\mathcal{D}_{\text{ERM}}$  for base training and  $\mathcal{D}_{\text{LEIA}}$  for adaptation. We find that across various ratios, LEIA’s performance remains strong in the setting with no information of group relevance (Table 12) and the setting with complete information of group relevance (Table 13).

## E. Theoretical Perspective on Low-rank Error Informed Adaptation

In this section, we provide a theoretical justification of why Low-rank Error Informed Adaptation (LEIA) works. Our goal is not to derive worst-case guarantees under explicit subgroup labels, but to formalize why restricting adaptation to a

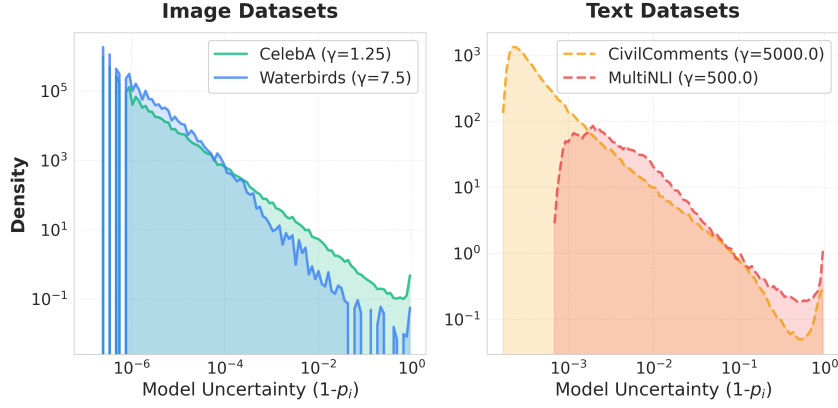


Figure 8. Differences in model uncertainty distributions by dataset, with image dataset having much higher density at very low probabilities and distinct tail of uncertain examples compared to compressed text datasets distributions.

Table 12. Performance comparison under varying  $D_{\text{ERM}}/D_{\text{LEIA}}$  ratios in the setting with no group information.

$D_{\text{ERM}}/D_{\text{LEIA}}$	WATERBIRDS		CIVILCOMMENTS	
	WGA	Avg Acc	WGA	Avg Acc
90–10	$88.8 \pm 0.3$	$92.3 \pm 0.4$	$70.2 \pm 0.3$	$91.0 \pm 0.9$
80–20	$90.1 \pm 0.1$	$93.7 \pm 0.7$	$71.6 \pm 0.7$	$91.4 \pm 0.4$
70–30	$88.8 \pm 0.3$	$92.3 \pm 0.4$	$70.9 \pm 0.1$	$91.1 \pm 0.8$
60–40	$88.8 \pm 0.3$	$92.3 \pm 0.4$	$71.0 \pm 0.8$	$91.1 \pm 0.8$
ERM	$69.1 \pm 4.7$	$84.1 \pm 1.7$	$63.2 \pm 1.2$	$85.4 \pm 0.2$

Table 13. Performance comparison under varying  $D_{\text{ERM}}/D_{\text{LEIA}}$  ratios in the setting with complete group relevancy information.

$D_{\text{ERM}}/D_{\text{LEIA}}$	WATERBIRDS		CIVILCOMMENTS	
	WGA	Avg Acc	WGA	Avg Acc
90–10	$89.4 \pm 0.3$	$92.8 \pm 0.9$	$72.2 \pm 0.7$	$91.4 \pm 0.4$
80–20	$90.1 \pm 0.1$	$92.8 \pm 0.9$	$72.9 \pm 0.2$	$90.9 \pm 0.8$
70–30	$89.4 \pm 0.3$	$92.3 \pm 0.4$	$72.0 \pm 0.3$	$91.3 \pm 0.5$
60–40	$89.2 \pm 0.3$	$92.5 \pm 0.6$	$71.7 \pm 0.2$	$91.3 \pm 0.4$
ERM	$69.1 \pm 4.7$	$84.1 \pm 1.7$	$63.2 \pm 1.2$	$85.4 \pm 0.2$

low-dimensional *error-informed subspace* yields an effective and stable correction mechanism under subpopulation shift.

### E.1. Error Geometry and Error-Weighted Covariance

Let  $e_{\hat{\psi}}(x) \in \mathbb{R}^d$  denote the frozen feature representation learned by the base model, and let  $c_{\hat{\phi}}$  denote the frozen classifier head such that  $f(x) = c_{\hat{\phi}}(e_{\hat{\psi}}(x)) \in \mathbb{R}^C$ . For each example  $(x_i, y_i) \in \mathcal{D}_{\text{LEIA}}$ , define the per-example loss  $\ell_i := \ell(f(x_i), y_i)$  and the corresponding LEIA weight  $\mu_i$ .

LEIA considers small additive linear-in-representation adjustments to the classifier head. Specifically, we consider perturbations of the form

$$\Delta f(x_i) = \Delta W e_{\hat{\psi}}(x_i), \quad \Delta W \in \mathbb{R}^{C \times d}.$$

Using a first-order Taylor approximation of the weighted empirical risk, the change in loss under such a perturbation is

$$\mathcal{L}(f + \Delta f) \approx \sum_i \mu_i \ell_i + \sum_i \mu_i \nabla_{f_i} \ell_i^\top \Delta W e_{\hat{\psi}}(x_i),$$

where  $\nabla_{f_i} \ell_i \in \mathbb{R}^C$  denotes the gradient of the loss with respect to the logits.

The first-order contribution can be written as

$$\sum_i \mu_i \nabla_{f_i} \ell_i^\top \Delta W e_{\hat{\psi}}(x_i) = \text{tr} \left( \Delta W \sum_i \mu_i e_{\hat{\psi}}(x_i) \nabla_{f_i} \ell_i^\top \right),$$

highlighting that effective updates should align with directions in representation space that are repeatedly associated with high loss.

To capture the geometry of such error-prone regions independent of class-specific gradients, LEIA computes the error-weighted covariance of representations

$$\Sigma_{\text{err}} = \sum_i \mu_i (e_{\hat{\psi}}(x_i) - \bar{e})(e_{\hat{\psi}}(x_i) - \bar{e})^\top, \quad \bar{e} = \sum_i \mu_i e_{\hat{\psi}}(x_i).$$

The leading eigenvectors of  $\Sigma_{\text{err}}$  identify directions along which high-loss examples exhibit the greatest shared variation, corresponding to latent error modes in representation space.

## E.2. Low-Rank Constrained Risk Minimization

LEIA restricts classifier adaptation to the span of the top- $k$  eigenvectors  $V_k \in \mathbb{R}^{d \times k}$  of  $\Sigma_{\text{err}}$ . The adapted logits take the form

$$f_{\text{LEIA}}(x) = f(x) + A^\top V_k^\top e_{\hat{\psi}}(x), \quad A \in \mathbb{R}^{k \times C},$$

which is equivalent to adding a rank- $k$  update  $\Delta W = V_k A$  to the classifier head.

The adaptation objective is

$$\min_A \sum_{(x_i, y_i) \in \mathcal{D}_{\text{LEIA}}} \mu_i \ell(f(x_i) + A^\top V_k^\top e_{\hat{\psi}}(x_i), y_i).$$

This restriction has three important properties.

1. *Spectral alignment*: The subspace  $V_k$  captures directions of maximal error-weighted variance, ensuring that updates focus on representation directions shared by many high-loss examples.
2. *Robustness without group labels*: Because  $\Sigma_{\text{err}}$  aggregates error structure across examples, LEIA targets latent error modes without requiring explicit subgroup annotations.
3. *Stability and efficiency*: Restricting adaptation to  $kC$  parameters prevents overfitting and catastrophic forgetting while preserving the base representation.

## E.3. Proposition: Spectral Optimality of the Error Subspace

**Proposition E.1** (Spectral Optimality). *Let  $\Sigma_{\text{err}}$  be the error-weighted covariance matrix. Among all  $k$ -dimensional subspaces  $V$  with orthonormal columns, the subspace spanned by the top- $k$  eigenvectors  $V_k$  maximizes*

$$\text{tr}(V^\top \Sigma_{\text{err}} V).$$

*Proof.* Let  $\Sigma_{\text{err}} \in \mathbb{R}^{d \times d}$  be symmetric positive semidefinite, and let its eigendecomposition be

$$\Sigma_{\text{err}} = U \Lambda U^\top,$$

where  $U = [u_1, \dots, u_d]$  is an orthonormal basis of eigenvectors and  $\Lambda = \text{diag}(\lambda_1, \dots, \lambda_d)$  with  $\lambda_1 \geq \lambda_2 \geq \dots \geq \lambda_d \geq 0$ .

For any matrix  $V \in \mathbb{R}^{d \times k}$  with orthonormal columns ( $V^\top V = I_k$ ), we can write  $V = UQ$  for some  $Q \in \mathbb{R}^{d \times k}$  with  $Q^\top Q = I_k$ . Then

$$\text{tr}(V^\top \Sigma_{\text{err}} V) = \text{tr}(Q^\top U^\top U \Lambda U^\top U Q) = \text{tr}(Q^\top \Lambda Q).$$

Writing  $Q = [q_1, \dots, q_k]$  with  $q_j \in \mathbb{R}^d$  and  $\|q_j\|_2 = 1$ , we have

$$\text{tr}(Q^\top \Lambda Q) = \sum_{j=1}^k q_j^\top \Lambda q_j = \sum_{j=1}^k \sum_{i=1}^d \lambda_i q_{ij}^2,$$

where  $q_{ij}$  denotes the  $i$ -th component of  $q_j$ .

Since  $\lambda_1 \geq \lambda_2 \geq \dots \geq \lambda_d$ , the above expression is maximized when each  $q_j$  places all its mass on the coordinates corresponding to the largest eigenvalues, subject to the orthonormality constraints  $Q^\top Q = I_k$ . This is achieved by choosing  $Q = [e_1, \dots, e_k]$ , where  $e_i$  are the standard basis vectors in  $\mathbb{R}^d$ .

Thus, the maximizer is  $V = UQ = [u_1, \dots, u_k] = V_k$ , the matrix of the top- $k$  eigenvectors of  $\Sigma_{\text{err}}$ , and the maximum value is  $\sum_{i=1}^k \lambda_i$ .

Therefore, the subspace spanned by  $V_k$  uniquely maximizes  $\text{tr}(V^\top \Sigma_{\text{err}} V)$  among all  $k$ -dimensional subspaces with orthonormal bases.  $\square$

#### E.4. Implications for Latent Subpopulation Shift

Consider any latent subgroup  $G \subseteq \mathcal{D}_{\text{LEIA}}$  whose mean deviation lies primarily in the span of  $V_k$ . Then LEIA admits a rank- $k$  head update that induces a first-order decrease in the average weighted loss over  $G$ . The magnitude of this decrease scales with the spectral mass of  $\Sigma_{\text{err}}$  captured by  $V_k$  and the alignment between subgroup gradients and the error subspace. If systematic errors arise from low-dimensional structure in representation space, LEIA provides a principled mechanism for correcting these errors using a constrained, stable, and group-agnostic adaptation.

## F. Additional related work

### F.1. Spurious Correlations

We elaborate on literature that has explored spurious correlations in particular. Deep learning models often exploit spurious correlations (Tu et al., 2020; McCoy et al., 2019)—features that are predictive on average but not causally related to the target label—leading to significant degradation in accuracy on certain subpopulations. Recent work has shown that such reliance on spurious features is quite common across various machine learning benchmarks (Salaudeen et al., 2025). These shortcut features can include image textures (Geirhos et al., 2020), background artifacts (Ribeiro et al., 2016; Beery et al., 2018), infrequent tokens in text (Wang et al., 2022; Du et al., 2023), or clinical heuristics in medical data (Zech et al., 2018; Winkler et al., 2019; Shahamatdar et al., 2024; Yang et al., 2024a). As a result, average accuracy may be high while performance on certain subgroups is unacceptably low. Models can also treat demographic attributes (e.g., gender or race) as spurious features that are correlated with the label in training data but non-causal, leading to systematic errors on minority subgroups (Zhao et al., 2017; Banerjee et al., 2023; Yang et al., 2024b). Several previous works have suggested methods to mitigate reliance on spurious correlation (Sagawa et al., 2020; Idrissi et al., 2021; Singla et al., 2022; Wang et al., 2020). Other works have suggested explanations for why spurious correlations are learned in ERM training (Nagarajan et al., 2024) and analyzing the representational spaces (Lu et al., 2024).

### F.2. Robust Learning with Group Attributes

When group or environment annotations are available, group-robust training methods optimize worst-group error (Sagawa et al., 2020), use group reweighting (Japkowicz, 2000; Kang et al., 2020), balanced sampling (Idrissi et al., 2021; Japkowicz, 2000; Zhang et al., 2017), retraining only the classifier head on a group-balanced validation set (Kirichenko et al., 2022; Rudner et al., 2024), and adopting domain-specific augmentations (Goel et al., 2020). In a similar vein, some methods aim to optimize a “Pareto-fair” objective, more general than simply the worst-group error (Balashankar et al., 2019; Martinez et al., 2020). However, these methods all rely on group annotations during training or validation, which may not be feasible in many settings. Moreover, these methods assume oracle knowledge of group importance.

### F.3. Robust Learning without Group Attributes

In settings where group labels are unavailable (Hashimoto et al., 2018), recent methods aim to identify and emphasize its failure modes by leveraging contrastive loss between hard examples (Zhang et al., 2022), discover latent group structure

(Sohoni et al., 2020), finds violations of the invariant risk minimization objective (Creager et al., 2021; Ahmed et al., 2021), or by semi-supervised learning to infer group attribute (Nam et al., 2020; Sohoni et al., 2020). Drawing on DFR, several other works have shown that retraining the last layer of the classifier can be effective without explicit group labels (Qiu et al., 2023; LaBonte et al., 2023). Our method, LEIA, shares this two-stage structure and optimizes in terms of the last layer but uniquely constrains adaptation to an error-informed low-rank subspace in the representation space. Besides the two stage paradigm, there are methods that rely on resampling and data attribution techniques (Kang et al., 2020; Jain et al., 2024).

#### F.4. Low-Rank Corrections

Our method also draws on prior work that established how biases can be mitigated with a few dimensions in transformers and vision language models (Zhao et al., 2025; Jang et al., 2025). These train-free or post-hoc debiasing studies identify small number of dominant latent directions capturing the biased signals (Chuang et al., 2023; Jung et al., 2024), and interventions along these directions can substantially reduce bias (Chuang et al., 2023; Gerych et al., 2024; Hirota et al., 2024; Jung et al., 2024; Zhang et al., 2025; Zhao et al., 2025; Jang et al., 2025). Additionally, parameter-efficient adaptation techniques such as low-rank updates (LoRA) (Hu et al., 2022) have shown that task- or subgroup-specific improvements can be achieved by updating only a small fraction of model parameters, avoiding the cost of full fine-tuning (Hu et al., 2022; Rimsky et al., 2024; Wu et al., 2024; Yin et al., 2024).